AN ABSTRACT OF THE THESIS OF

Prakash Mugdur for the degree of Master of Science in Chemical Engineering presented on March 11, 2005.

Title: Continuous Flow Microreactor for Chemical Bath Deposition: A Novel Approach to the Deposition of Polycrystalline Semiconductor Thin Films.

Abstract approved:

Redacted for Privacy

Chih-Hung Chang

Over the years, chemical bath deposition (CBD) is being widely used in the fabrication of Cu (In, Ga) Se_2 and CdTe based solar cells and photovoltaics. Many chalcogenides have been successfully deposited by this technique and it has received a great deal of attention owing to its low temperature and low-cost nature. CdS, an important layer in heterojunction solar cells and other optoelectronic devices, has been successfully deposited by this technique, which is normally carried out as a batch process. But a major disadvantage of batch CBD is the formation of particles and also unwanted deposition generating a lot of waste and thus resulting in defective devices.

In this study, we have developed a continuous flow microreactor for CBD to overcome the drawbacks of batch process. This novel microreactor setup makes use of a micromixer for efficient mixing of the reactant streams and helps in

controlling the particle size and distribution before the solution impinges on the hot substrate.

CdS semiconductor thin films were successfully deposited on oxidized silicon substrates using the microreactor setup and a batch reactor as well. Comparisons of nanostructured thin films were performed by various characterization techniques. The surface morphology of the deposited films, carried out by AFM, SEM and Dektak surface profiler, clearly indicated an improved film quality in case of microreactor. This setup can also be used to deposit various other compound semiconductor thin films with improved film quality and minimum waste production.

© Copyright by Prakash Mugdur
March 11, 2005
All Rights Reserved

Continuous Flow Microreactor for Chemical Bath Deposition: A Novel Approach to the Deposition of Polycrystalline Semiconductor Thin Films

by
Prakash Mugdur

A THESIS

submitted to

Oregon State University

in partial fulfillment of
the requirements for the
degree of

Master of Science

Presented March 11, 2005
Commencement June 2005

Master of Science thesis of Prakash Mugdur presented on March 11, 2005.

APPROVED:

Redacted for Privacy

Major Professor, representing Chemical Engineering

Redacted for Privacy

Head of the Department of Chemical Engineering

Redacted for Privacy

Dean of the Graduate School

I understand that my thesis will become part of the permanent collection of Oregon State University libraries. My signature below authorizes release of my thesis to any reader upon request.

Redacted for Privacy

Prakash Mugdur, Author

ACKNOWLEDGEMENTS

I express my sincere gratitude and heartfelt appreciation to Dr Chih-Hung Chang for the enormous support and invaluable guidance he provided during the last two years. I am greatly indebted to Dr Chang for his stimulating suggestions and kind words of encouragement that helped me all through this research and during the writing of this thesis. A couple of years ago, when my options were open to a dual master's degree in chemical engineering and computer science and when I was a little confused in finding out where exactly my interests are, it was Dr Chang and his research work that attracted me towards this fascinating area of chemical engineering i.e. thin film processing and semiconductors. I would always be grateful to him for having shown me this way and for providing an opportunity to work under him on this wonderful project which is supported by the National Science Foundation's Process & Reaction Engineering program under a CAREER grant # CTS-0348723.

I would like to thank Dr Goran Jovanovic for showing interest in my academic progress all through these years and also for serving in my graduate committee. His timely advice and guidance will always be remembered. Thanks to Dr Bella Bose, my minor advisor, for his many friendly enquiries on my academics and research activities. To Dr Claudia Maier, who kindly agreed to act as Graduate Council Representative.

I would like to express my gratitude to all those who gave me the possibility to complete this thesis. Special thanks are due to: Dr Philip Watson for his timely assistance with AFM measurements; Dr Augusto Morrone for his valuable assistance in TEM measurements; Dr Cheol-Hee Park for his assistance in XRD measurements; for people in Pohang University and Yeungnam University in Korea for their help in XPS and SEM analysis.

I feel deeply indebted to my parents back home in India. Their love and moral support in all these years have given me enough strength to carry on with any tough task. I had a great time here in Oregon State University and the memories of this lovely school will be cherished forever. The help and encouragement from all the people in the department of chemical engineering and elsewhere in the university will be remembered for a long time to come.

The chain of my gratitude will definitely be incomplete if I forget to thank the first cause of this chain, in Aristotle's words, The Prime Mover. My deepest and sincere gratitude for inspiring and guiding this humble being.

TABLE OF CONTENTS

TABLE OF CONTENTS (Continued)

LIST OF FIGURES

LIST OF FIGURES (Continued)

LIST OF TABLES

LIST OF APPENDICES

LIST OF APPENDIX FIGURES

Continuous Flow Microreactor for Chemical Bath Deposition: A Novel Approach to the Deposition of Polycrystalline Semiconductor Thin Films

CHAPTER 1

INTRODUCTION

In recent years, metal chalcogenide semiconductors have received intensive attention in electronic and optoelectronic applications for use in semiconductor lasers and infrared detectors as well as quantum dot structures. Typically, metals like Cd, Zn, Pb, Cu etc. are deposited as sulfide, selenide or telluride [14]. There has been a growing enthusiasm, over the recent years, for developing these (and such other new) polycrystalline thin film semiconductors using a variety of techniques such as electrodeposition, vacuum evaporation, screen printing, spray pyrolysis, sputtering, chemical vapor deposition (CVD) and chemical bath deposition (CBD).

Among them, chemical bath deposition has received a special significance owing to its low temperature and low cost nature. Many chalcogenide semiconductors have been successfully deposited using this technique. It is being used for a long time for preparing thin films of CdS, an important component of heterojunction solar cells and other electrooptic devices.

CBD is generally regarded as the solution analogue of CVD. In fact, CBD has many similarities to CVD, the most important one being the heterogeneous surface reaction common to both the techniques. The fundamental growth mechanism in CBD is very similar to that of CVD and follows the same basic steps of thin film growth viz. adsorption (physisorption) of atoms/molecules, surface diffusion, chemisorption, nucleation and growth. It provides a simple and inexpensive way of producing uniform, adherent and reproducible large-area thin films for thin film electronic applications such as solar cells and thin-film transistors (TFTs) [1].

The main benefit of CBD over other deposition techniques (mentioned earlier) is the ability to deposit a number of materials directly onto a substrate. Also, the starting material does not have to be very pure, provided the impurities are soluble. In case of CVD, assumed to be the best known deposition technique, the main disadvantages are its need for vacuum and a high temperature for operation. On the contrary, CBD can be carried out at atmospheric pressure under low temperatures (close-to-room temperature).Maintaining a vacuum is always expensive which in turn makes CVD an expensive process compared to CBD. For these reasons, CBD has already been proved to be a very useful method in large area devices such as computer monitors and high efficiency $CuInSe_2$ and CdTe solar cells [2].

Though CBD has many advantages as mentioned above, still it suffers from some of the drawbacks. In case of batch CBD process, the heat needed for

chemical reaction is supplied from the solution bath to the sample surface, resulting in heterogeneous CdS nucleation at the surface and homogeneous CdS formation in the bath. Thus, for baths heated by thermal jacket (glass beaker etc.) or water bath, significant CdS deposition also occurs on the walls of the vessels. Added to this, the bath should be stirred vigorously to ensure uniform thermal and chemical mixing and to minimize sticking of homogeneously nucleated CdS particles to the growing film surface. Also, the unequal volumes of the bath used to form the desired CdS film generates a lot of waste and creates defects in devices. Although efforts have been made by various group of researchers to reduce the bath-to-surface volume with the use of cover plates [3], yet a comprehensible path for combining large area deposition with high utilization and growth rate for high conversion efficiencies has not yet been demonstrated.

The focus of this research is to develop a continuous flow microreactor (CFM) to overcome the above mentioned drawbacks associated with batch CBD process. This novel reactor provides the benefit of introducing fresh quantity of reactant solutions to the system (continuous process) that allows strict control over the particle size and its distribution before the product solution impinges on the hot substrate.

Mixing on microscopic scale is quite difficult. Although diffusion is fast, the Reynolds number is generally low and hence the flow is laminar. The efficiency of mixing between two fluids is directly related to the interfacial area between them. In the absence of turbulence, it is difficult to increase the interfacial

area of contact through which the molecules diffuse. Our new setup makes use of interdigital micromixer for efficient mixing of the reactant streams. CFM also helps in differentiating the molecule-by-molecule growth from the cluster-by-cluster growth (this aspect of the project is treated as future work). Also, it is believed that the new microreactor setup would help in better understanding of the particle formation and deposition processes in CBD.

CHAPTER 2

REVIEW OF CBD

Chemical bath deposition (CBD) of thin films finds it origin more than a century ago (in 1835) when Liebig reported the deposition of silver (the silver mirror deposition) using a chemical solution technique [37]. The first reported deposition of a compound semiconductor film was the formation of "lusterfarben" (meaning lustrous colors) on metals from thiosulphate solutions of copper sulfate, lead acetate and antimony tartrate which resulted in "splendid" colored films of CuS, PbS and SbS respectively [38].

In 1884, J.E.Reynolds reported that thiocarbamide (or "sulfur urea"), a source of sulfur, could be easily desulfurized by certain metallic oxides and hydroxides to form the corresponding sulfides [4]. He observed that when thiocarbamide was heated in basic solution of lead hydrate, lead sulfide separated in a galenoid form and got firmly attached as an adherent specular layer on the sides of the vessel. The process initially started with appearance of brownish coloration when the temperature was around 40°C and the solution turned turbid at around 45°C and a specular layer began to form on the sides and at the bottom of the vessel when the temperature reached around 50°C. This can be traced as the first attempt to deposit a material on the surface of a substrate and the process, which is the solution equivalent of chemical vapor deposition (CVD), is being

called CBD or chemical solution deposition (CSD). But as compared to CVD which is widely used in semiconductor industries, the development of CBD has remained limited.

Infrared photoconductivity of CBD PbS was reported a century ago [39, 40] and this has led to subsequent investigations in lead chalcogenide films. The first application of CBD dates back to early 1940's (during World War II) when it was used for depositing PbS films in the presence of thiourea (thiocarbamide) and subsequent fabrication of infra-red photoconducting detectors [5]. Also, n-p junctions were formed by using the appropriate dopants in the solution bath [6].

For a long time, CBD was only limited to PbS and PbSe films. It was only in 1961 that the deposition of CdS was reported by Mokrushin *et al.* [41]. They deposited CdS from a thiosulphate solution. During the mid 1960's, Kitaev and co-workers, a group of Russian researchers, did extensive work on thin film deposition of CdS films based on the PbS deposition technique [7] and proposed a growth mechanism taking into account the formation of colloidal particles and their subsequent adsorption on a surface. They believed that for the decomposition of thiourea to begin, a solid phase, e.g. $Cd(OH)_2$, must be present in the working solution and that CdS films can only be produced in the presence of this solid phase.

Kaur *et al.* [13] studied the kinetics of CdS growth from basic solution. They found that the films prepared in the presence of Cd $(OH)_2$ in the solution were strong and adherent and that vigorous stirring of the solution would decrease

the powdery nature of films and increase adhesion. They concluded that the higher deposition rate would result in lower terminal thickness.

Nair et al. [43] prepared CdS films of very high photoconductivity (p/d >9) by controlling the molar ratios of Cd^{2+} and thiourea. They found that the films produced by equimolar ratios were of low quality.

Nair and Nair [44] carried out deposition directly under sunlight using cadmium acetate and thiourea at room temperature. During the initial stages of deposition, they observed a darkening of the bath which increased the solar radiation absorption of the bath. This photothermal reaction in the bath increases the bath temperature and thus increases the rate of deposition. Good quality films showing excellent optoelectronic properties were obtained.

A number of dopants were added to CdS films during their preparation as demonstrated by a number of researchers. Bharadwaj et al. [45] prepared films by doping CuI and $AlCl_3$ in the reaction bath. Sahu et al. [46] deposited Li doped films by adding Li_2O_3 in the bath. The optical bandgap of such a film was 2.35 eV and the resistivity was lower. Bargale et al. [47] made Na doped CdS films by adding sodium sulphate to the solution bath. They observed that the addition of Na reduced the crystallinity of the films. Also, copper doped films were produced by Pavaskar et al. [48] by doping CuI in the bath. They observed that the addition of cations like Cu, In, Zn etc. to the reaction bath would make films amorphous. Lastly, Warad et al. [49] produced CdS films by adding bismuth nitrate in the bath. They noted that the thickness of the doped films increased with doping levels.

Later on, thiourea was replaced by its selenium analogues, like selenourea and dimethylselenourea, and this marked the beginning of the fabrication of a series of various selenide compounds, the first compound being PbSe [8]. CBD was then initiated for other sulfides such as CdS [9] and Ag_2S [10] during this period. An extensive review by Chopra and co-workers [11] suggests that about 20 different compounds were synthesized by CBD in 1982. But no technique-compound combination has gained as much attention and recognition as CBD CdS since CBD displays superior qualities when compared to classical vapor phase deposition techniques for the fabrication of high efficiency solar cells for the extension to large area processing. CdS also emerges in integrated microelectronics as interface passivation layer in III-V MISFET devices [12].

A review worth mentioning at this stage is the deposition of CdS films reported by Lokhande [50]. He used the more uncommon acidic bath with sodium thiosulphate as a source of sulfur (instead of thiourea). Equimolar amounts of $CdSO_4$ and $Na_2S_2O_3$ solutions were mixed and heated to 85 °C for about 20 mins. As the bath was acidic, the pH was around 2-3. He observed yellowish CdS films deposited on glass. The bath was further heated to 150 °C which improved the adherence of films.

More recently, Boyle *et al.* [51] also used acidic bath containing $CdCl_2$, urea and thioacetamide to deposit CdS films. They heated the solution bath to 70-80 °C maintaining its pH around 5.5-4.9 (using 5 M HCl or NaOH).

Of all the semiconductor materials, CdS has been the most studied one and many papers have been published and a broad range of deposition conditions have been explored over the past two decades. Ammonia baths are most commonly used since ammonia acts as a very efficient complexing agent for Cd ions and helps maintain the pH in basic conditions as required by the reaction [13, a2, 15, a6, a13, a15]. Few other complexing agents such as triethanolamine [a3], ethylenediamine [a14] and nitrilotriacetate [a13] have also been tried. As for the source of sulfur, thiourea has been the most commonly used one but other compounds like thioacetamide [a8, a11, a10, a17] and allylthiourea [15] were also used for the deposition. A detailed review of chemical deposition of various chalcogenides including binaries and ternaries of sulfide and selenide compounds was done by Lincot *et al.* [24]. They have given an extensive analysis of the basic aspects of deposition along with the growth kinetics mechanisms involving quartz crystal microbalance (QCM) and impedance measurements. Finally, they have described the epitaxial growth of various semiconductors. Epitaxial growth of CdS has also been demonstrated. A thorough literature review on chemical bath deposition of CdS and other important semiconductor materials such as Ag_2S, PbS, ZnS and CdSe is compiled in Appendix A.

Chemical deposition received much attention after it was shown that CdS films, chemically deposited onto CdTe films, could be used to make superior photovoltaic cells (PV) compared with the earlier evaporated CdS. The first successful application of such CBD CdS films in PV cells was reported by Uda *et*

al. [42]. Later on, many people followed this trend by making high efficiency $CuInSe_2$ cells. Nowadays, CdS layer is almost universally used on both CdTe and $CuInSe_2$ thin film PV cells.

The deposition process described so far, from the literature, is a batch CBD process. A unique method of depositing CdS films was reported by McCandless *et al.* [23]. In this process, called Chemical Surface Deposition (CSD), a solution containing the desired reactants was applied to a preheated surface. The heat from the substrate acted as a source of energy needed for reaction at the surface, resulting in heterogeneous nucleation. In this case, heterogeneous nucleation was favored over homogeneous precipitation resulting in a higher percentage of cadmium in the film. Moreover, the CdS thin films produced by this technique exhibited negligible occurrence of pinholes and particulates.

In this section, our discussion has been primarily focused on some of the most important surveys from literature regarding the deposition conditions and methods used by various group of researchers in respect of different chalcogenides and CdS in particular. A detailed discussion on various growth mechanisms from literature and our current understanding of CBD CdS is provided in chapter 4 of this document.

In this work, we have developed a novel continuous flow CBD microreactor to control thin film micro and nano structures based on CBD process. No work has been reported in the literature about such a technique or the reactor,

which makes use of microreaction technology to produce nanocrystalline thin films.

CHAPTER 3

EXPERIMENTAL METHODS

The following sections describe the experimental conditions and setup used for our batch and continuous flow microreactor (CFM). In both cases, oxidized silicon substrates (silicon wafer coupons) measuring 15 x 10 mm were used for deposition studies. The coupons were initially sonicated in an ultrasonic bath using 1M NaOH (Mallinckrodt) for about 10-15 min. and then cleaned according to standard AMD (Acetone, Methanol, DI water) procedure. Finally, they were dried under a stream of nitrogen gas before being used in the process. The chemical waste solutions, produced during the reaction, were handled according to MSDS requirements.

For the purpose of our experimental studies, 0.004 M cadmium chloride solutions were prepared using anhydrous $CdCl_2$ (Fluka Chemika), 0.04 M ammonium chloride solutions were made using NH_4Cl (Fisher Chemicals) and 0.04 M thiourea [$SC(NH_2)_2$] solutions were prepared using 99% thiourea (Aldrich Chemicals).Also, 0.4 M ammonium hydroxide (EM Science) solution was used directly for the process. All solutions were prepared using Millipore (18.2 MΩ .cm) water and mass of the chemicals measured using a Scientech SP1000 Model 13855 analytical balance. The solutions were prepared, at room

temperature, inside the hood with continuous stirring using magnetic stir bar to ensure complete dissolution of the reagents used.

3.1 Experimental Setup

3.1.1 Batch Reactor

CBD batch reactor consisted of an 800ml glass beaker mounted on top of a VWR hotplate stirrer. The recipe consisting of various reactants and their volume used for our experiments is shown in the table 3.1:

Table 3.1 Recipe for batch CBD

Reactants	Vol (ml.)
H_2O	436
$CdCl_2$	60
NH_4Cl	20
$SC(NH_2)_2$	60
NH_4OH	24
Total	**600**

The coupons were taped on to a 75 x 25 mm commercial glass slide after cleaning by AMD procedure, as mentioned in section 3.1, and immersed in 436ml. of DI water taken in the beaker. $CdCl_2$ (60ml.) and NH_4Cl (20ml.) were added slowly with stirring and the temperature of the reaction mixture was monitored using a thermometer. When the temperature reached 80°C, thiourea was added and the addition of thiourea decreased the temperature. The heating was continued until the reaction mixture reached 80°C again and NH_4OH (28ml.) was added at

this time to begin the reaction. The reaction was allowed to go for different periods of time (5min, 10min etc.) and then the coupons were taken out of the solution, removed from glass slide, washed with DI water and dried under a stream of nitrogen. Figure 3.1 shows the experimental batch reactor used for our studies.

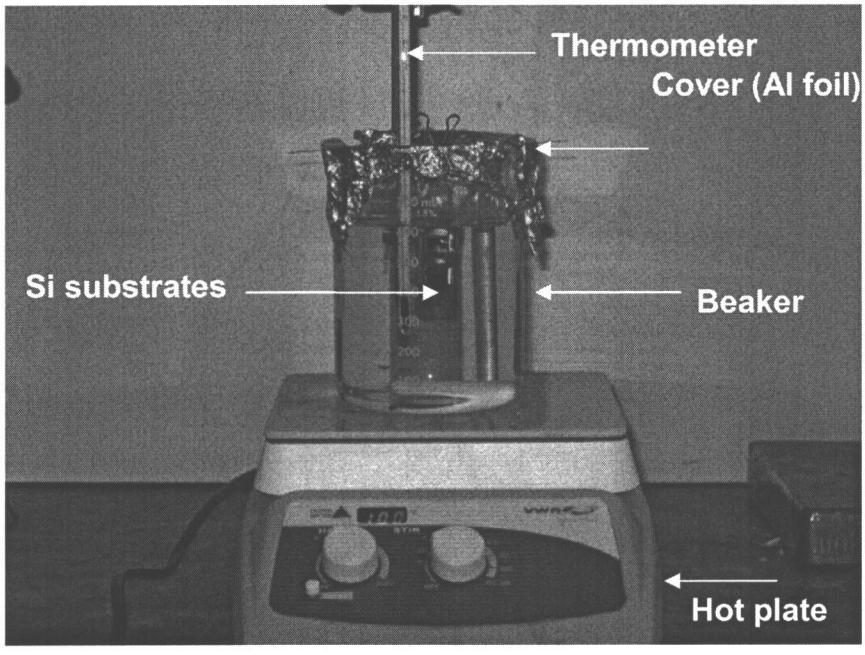

Figure 3.1 CBD batch reactor

3.1.2 Continuous Flow Microreactor

The Continuous Flow Microreactor (CFM) used in our experiments basically consisted of two syringe pumps and a micromixer. They were connected using PEEK tubing (1/16" OD, 0.03" ID from Upchurch Scientific) as shown in

Figure 3.2. The recipe consisting of various reactants and their volume used for our experiments is shown in the table 3.2:

Table 3.2 Recipe for CBD (CFM)

Stream A	**Vol (ml.)**	**Stream B**	**Vol (ml.)**
$CdCl_2$	12	H_2O	13
NH_4Cl	10	$SC(NH_2)_2$	12
NH_4OH	2	**TOTAL**	**25**
TOTAL	**24**		

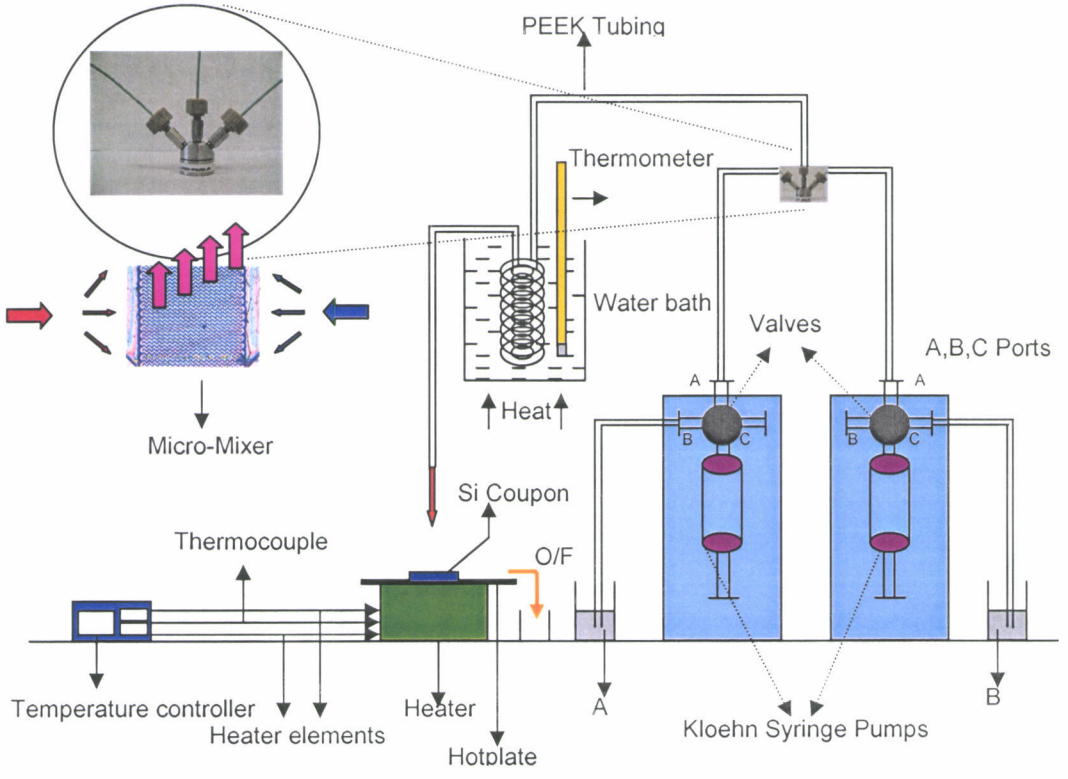

Figure 3.2 Schematic of Experimental Setup (CFM)

Two syringe pumps (V6 module from Kloehn Ltd.) of 25ml. each were used for holding reactant streams A and B before mixing. Each pump has three ports (A, B, C) as shown in figure 3.3. One port of each pump was used for aspirating the reactant streams and port A (usually) was used for dispensing the same.

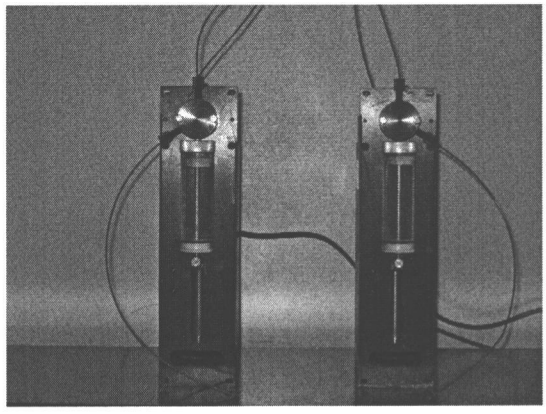

Figure 3.3 Kloehn syringe pumps

The standard slit interdigital micro mixer (SSIMM from Institut für Mikrotechnik Mainz, Germany) was used for our experimental studies. It is essentially made of stainless steel SS 316Ti housing with inlay of thermally oxidized silicon (30 μm x 100 μm channels). These mixer inlays are fabricated by LIGA technique or additionally by advanced silicon etching (ASE).Figure 3.4 shows micromixer and its top and bottom housing with inlay.

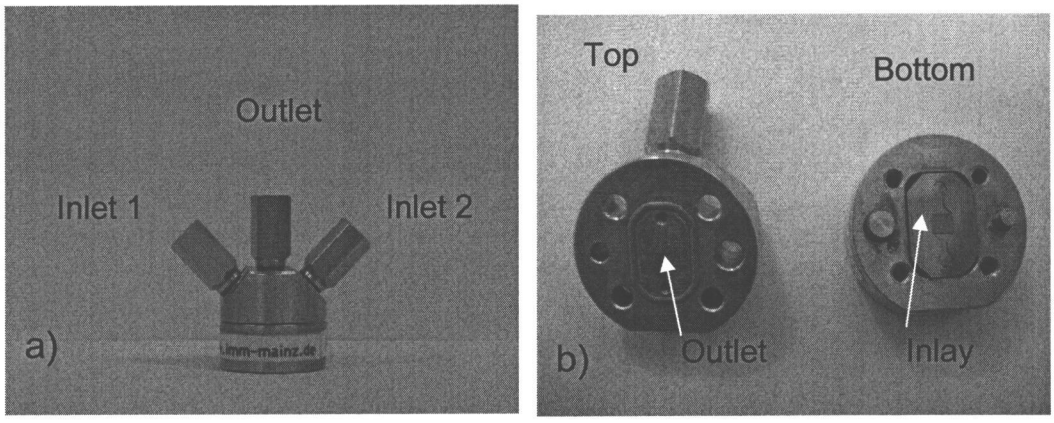

Figure 3.4 (a) Micromixer and (b) its top and bottom housing

The micromixer is a prototype version specially designed for fast mixing of fluids. The mixing elements are equipped with an interdigital microchannel configuration with corrugated walls which help in fast mixing by diffusion. The reactant streams (A and B in our case) are introduced into the mixing element as two counter-current flows which stream into interdigitated channels with corrugated walls. For our present studies, mixing element with channel width of 30 um was used and the typical values range from 20 to 50 um. By means of the slit-shaped interdigital microchannels a flow lamellae of the two fluids to be mixed is generated. This lamellated flow leaves the interdigital channels perpendicular to the direction of the feed flow. Since the thickness of each substream is small, this results in fast mixing through diffusion. Additionally, the corrugated shape of the channel walls helps increase the contact surface of the substreams thus improving the mechanical stability [36]. Also, the laminar flow in microchannels would

greatly reduce the possibility of particle collisions and hence the growth of particles through coagulation.

For our experimental operations, the reactant streams A (24ml.) and B (25ml.) were initially pumped into syringes and then they were dispensed through the PEEK tubing and allowed to mix in the micromixer. The resulting product, from micromixer, was passed through a 5' long coil (PEEK), kept immersed in a hot water bath maintained at 80-85°C (using VWR hot plate stirrer). The solution was made to impinge on the coupon, taped to a 3" dia. SS metallic plate and heated on a hotplate (2" dia. x 0.75" thick SS disk from Watlow) at 80-90°C. The syringe pumps were operated at a speed of 250 steps/sec. (Hz) and the time taken for the deposition, at this speed, was about 3.12mins. Once the process was completed, the coupon was removed from the plate, washed with DI water (Millipore) and dried under a stream of nitrogen gas. Figure 3.5 shows a picture of the experimental setup.

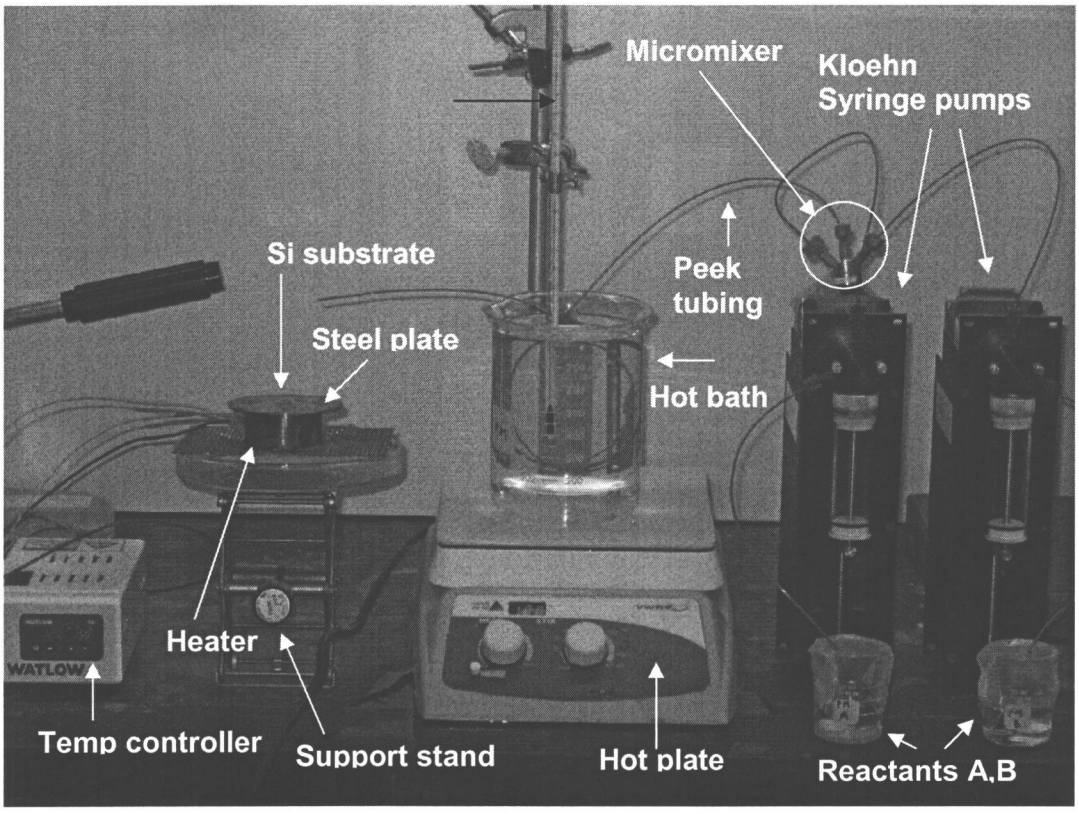

Figure 3.5 Experimental Setup (CFM)

3.2 Methods of Analysis

Both batch reactor and continuous flow microreactor were used for depositing CdS. The deposited films were characterized by transmission electron microscopy (TEM) along with selected area electron diffraction (SAED) and energy dispersive X ray (EDX), X ray photoelectron spectroscopy (XPS), X ray diffraction (XRD), atomic force microscopy (AFM) and scanning electron microscopy (SEM). 3-D mapping of films was done (Dektak 8 stylus profiler) to further confirm the surface morphology.

3.2.1 TEM

When a sample is illuminated with a beam of high-energy electrons (~ 100-400 keV) under high vacuum, some electrons are scattered and some pass through the sample. The resulting diffraction pattern consists of a transmitted beam and a number of diffracted beams and they can be captured on a fluorescent screen. The diffraction pattern gives the lattice spacing values (d-spacing) for the structure under consideration. Alternatively, by using the transmitted beam, magnified image of the sample can be produced on the viewing screen. Also, by allowing the transmitted beam and one or more of diffracted beams to recombine, we can obtain high-resolution image containing information about the atomic structure of the specimen. After the interaction with the sample, the electron beam loses energy and in turn characteristic X-rays are emitted by the atoms in the sample. These characteristic X-rays can be detected and analyzed to produce EDX spectrum which gives details of the local chemistry of the material [27].

TEM technique was employed for direct observation and comparison of crystalline samples of CdS produced by batch and CFM methods.

For TEM, SAED and EDX studies, the depositions took place on copper grids covered with a thin film of carbon (Lacey carbon type-A, 300M copper, #01890 from Ted Pella). To prepare samples, in case of batch reactor, drops of CBD solution were taken out of the beaker at specified time intervals and loaded onto copper grids kept on a glass slide and then filter paper was used to absorb fluid through the bottom of the grid. In case of CFM, the copper grids were taped

onto glass slides and the deposition was done using impinging flow for different periods of time. Later, the grids were carefully removed from glass slides. In both cases, the grids were finally stored in TEM grid storage box (#160 from PELCO) before being sent for analysis.

Measurements were done, with assistance from Dr. Augusto Morrone, using a JEOL 2010F field emission gun TEM operated at 200KV, equipped with a Noran Vantage EDXS system that was used for the composition analysis.

3.2.2 XPS

XPS, also called electron spectroscopy for chemical analysis (ESCA), is a technique which provides information about the chemical state and concentration of elements present on the outermost layers of a solid surface. When a material is exposed to photons of known energy, photoelectrons are emitted from the material. The energy of these emitted photoelectrons is given by the relation:

$$E_{ke} = h\upsilon - E_{be} - \phi$$

where E_{ke} and E_{be} are the kinetic and binding energies of a specific core or valence level electrons respectively, $h\upsilon$ is the characteristic photon energy of source and ϕ is a parameter specific to the spectrometer in use. These photoelectrons originate from specific electronic energy levels associated with the atoms in the analysis volume. Depending on the ionization which may occur in any shell for a particular atom, the obtained spectrum for that element will consist

of various peaks corresponding to electron emission from different shells [27]. For each and every element, there will be a characteristic binding energy associated with each core atomic orbital i.e. each element will give rise to a characteristic set of peaks in the photoelectron spectrum at kinetic energies determined by the photon energy and the respective binding energies. The presence of peaks at particular energies therefore indicates the presence of a specific element in the sample under study [28].

The XPS technique was used to investigate the presence of various elements on the surface of the as-deposited as well as annealed CdS thin films.

The samples were prepared on silicon wafer coupons in the usual manner and the same were used for analysis. One set of samples were annealed, in a vacuum oven at 200°C for 30min., before analysis and the other set was analyzed without annealing in order to observe the effect of annealing on samples.

The XPS measurements were performed using a VG ESCALAB 220-IXL (VG Scientific 1998) instrument with Mg-Kα radiation of photon energy 1253.6 eV at Pohang University in Korea.

3.2.3 XRD

When X-ray passes through matter, the radiation interacts with the electrons in the atoms, resulting in scattering of the radiation. In case of crystalline matters, the atoms are organized in planes and the distances between the atoms are of the same magnitude as the wavelength of the X-rays and hence constructive and

destructive interference will occur. This results in diffraction where X-rays are emitted at characteristic angles based on the spaces between the atoms organized in crystalline structures called planes. Most crystals can have many sets of planes passing through their atoms. Each set of planes has a specific interplanar distance and gives rise to a characteristic angle of diffracted X-rays. The relationship between wavelength, atomic spacing (d) and angle is given by Bragg Equation. If the illuminating wavelength is known and the angle can be measured (with a diffractometer) then the interplanar distance can be calculated from the Bragg equation. A set of'd-spaces' obtained from a single compound will represent the set of planes that can be passed through the atoms and can be used for comparison with sets of d-spaces obtained from standard compounds. The simplest way of doing this is the direct comparison of the diffraction patterns with the standard X-ray data file published by the joint committee on powder diffraction standards (JCPDS).

The XRD measurement was used to obtain information on the phase as well as the crystalline orientation of CdS film deposited by CFM.

A thick layer of CdS (2500-3000 A) was deposited on silicon coupon and the sample was then analyzed using Siemens D-5000 X-ray diffractometer (using copper k-alpha radiation with a wavelength of 1.5418 A on high resolution mode) available in the dept of chemistry at Oregon State University with the assistance from Dr. Cheol-Hee Park.

3.2.4 AFM

An Atomic Force Microscope (AFM) consists of an extremely sharp tip mounted or integrated on the end of a tiny cantilever spring which is moved by a mechanical scanner over the surface to be observed. Every variation of the surface height varies the force acting on the tip and therefore causes the deflection of the cantilever. This deflection is measured by an integrated sensor at the base of the cantilever spring and recorded line by line in the electronic memory [34].

AFM measurement was done in order to characterize and compare the surface morphology of CdS films produced by batch and CFM.

For the purpose of analysis, the samples produced in the usual manner were cut into 1cm x 1cm size coupons and glued onto thin metallic discs (~ 1.5 cm dia).

Measurements were performed using a Digital Instruments (DI) Nanoscope III in contact mode with the help of Dr Phillip Watson in the dept of chemistry at Oregon State University.

3.2.5 SEM

The SEM is primarily used in the study of surface topography of solid specimens. Because of its enhanced depth of field, it is often preferred in place of optical imaging system. In case of SEM, a focused beam of electrons (typically 30 keV), passing through an evacuated column, is swept over the surface of a sample and the resulting emissions from the sample (X-rays, backscattered electrons, secondary electrons) are detected. A three-dimensional image of the specimen is

formed on cathode ray screen by mapping the intensity of the detected signal as a function of position. Also, by energy analysis of the emitted X-rays it is possible to obtain details of local chemistry of the sample [35].

SEM analysis was carried out in order to investigate the surface morphology of CdS thin films produced by batch and CFM. The CdS films were grown on silicon coupons and the same were used for analysis. The analysis was done using S-4100 (Hitachi Ltd.) FE-SEM with a cold type field emission electron gun as source at Yeungnam University in Korea.

CHAPTER 4

RESULTS AND DISCUSSION

It is necessary to understand the basic terminologies of CBD deposition process in order to better understand the growth mechanisms involved. A brief theoretical background is given at the beginning of the chapter followed by various growth mechanisms proposed by several researchers. Based on this, our current understanding of CBD CdS mechanism has been described. Lastly, various characterization results of CdS thin films grown by batch reactor and continuous flow microreactor (CFM) are discussed with a detailed analysis and comparison of both processes.

4.1 Theoretical background of chemical deposition

Solubility and Ionic product

An important concept for understanding the mechanism of CBD is that of solubility product. The solubility product gives the solubility of a sparingly soluble ionic salt [25]. On dissolving a sparingly soluble salt, say MN, in water, a solution containing M an N ions in contact with the undissolved solid MN is obtained. At saturation, equilibrium is reached between the two.

Thus, $MN\ (s) = M^{+} + N^{-}$

On applying law of mass action at equilibrium,

$$k=\frac{C_{M^+}C_{N^-}}{C_{MN(s)}}$$

where C_{M^+} ,C_{N^-}, C_{MN} are the respective concentrations of M, N, and MN in the solution.

Since the concentration of a pure solid phase is constant, we can write

$C_{MN(s)}$ = a constant= k'

$$\text{Thus, } k=\frac{C_{M^+}C_{N^-}}{k'}$$

Or $kk' = C_{M^+}C_{N^-}$

Product of two constants is a constant and hence we can write

$ks = C_{M^+}C_{N^-}$ where ks= kk'

The constant ks is called solubility constant and the product $C_{M^+}C_{N^-}$ is called ionic product. When a solution is saturated, the solubility product is equal to the ionic product. When the ionic product is less than the solubility product, the solution will be in unsaturated condition. Thus, it follows that when the ionic product exceeds the solubility product, a condition called supersaturation is reached. In most cases, the precipitation occurs at this condition. This condition is very important from the view of chemical deposition process as discussed later [50].

Nucleation process

Chemical deposition can occur either by homogeneous nucleation in solution bath or by heterogeneous nucleation on the surface of a substrate. In case of homogeneous nucleation, the new phase is formed in a solution having no foreign phases initially. The first stage in the growth is the formation of embryos (nuclei) by collision between individual ions or molecules. These embryos grow by collision with the other individual species such as ions, atoms or molecules. But in case of chemical deposition, adsorption of ions on the surface of embryo appears more likely to be the growth mechanism. On the contrary, heterogeneous nucleation is due to the presence of a foreign interface on which the growth takes place. Here the embryos can adsorb onto the substrate surface.

4.2 Growth mechanisms of CBD

With this theoretical background, we can now move on to the actual growth kinetics related to CBD. Although various groups of researchers have proposed mechanisms related to chemical deposition, yet it is an open topic in the literature.

The initial kinetics studies by Kaur *et al.* [13] suggests that the growth of CdS films takes place either by ion-by-ion condensation of Cd^{2+} and S^{2-} or by the adsorption of colloidal CdS formed in the solution. They also suggested that the ion-by-ion growth mechanism results in thin, hard, adherent and reflecting films,

whereas the colloidal adsorption results in thick, powdery and reflecting films. According to their mechanism, Cd^{2+} forms due to dissociation reaction:

$$CdSO_4 \rightarrow Cd^{2+} + SO_4^{2-}$$

In the presence of ammonium hydroxide, the following equilibrium reaction takes place:

$$NH_4^+ + OH^- \longleftrightarrow NH_3 + H_2O$$

Cd^{2+} ion then complexes with ammonia, thus controlling the concentration of free cadmium ions:

$$Cd^{2+} + nNH_3 \longleftrightarrow Cd(NH_3)_n^{2+}$$

The following reactions show the hydrolysis of thiourea, releasing free sulfide ions:

$$SC(NH_2)_2 \longrightarrow H_2S + CN_2H_2$$

$$H_2S + 2OH^- \longleftrightarrow 2H_2O + S^{2-}$$

Free cadmium ions then react with free sulfide ions to form CdS:

$$Cd^{2+} + S^{2-} \longrightarrow CdS\ (s)$$

When the ionic product exceeds the solubility product of CdS ($\sim 10^{-25}$) it precipitates in the bulk of the solution as colloids (homogeneous formation) or at the surface of the substrate as film (ion-by-ion process).

However, study conducted by Lincot *et al.* [15], using quartz crystal microbalance (QCM), suggests that this growth mechanism is more likely to be the one for the homogeneous nucleation rather than the heterogeneous one. According

to their studies, three main phases were evidenced during the growth of CdS films by CBD:

- The induction/coalescence range
- The compact layer growth range
- The porous layer growth range

During the induction period, the growth rate of film is slow. This region corresponds to short reaction times and is marked by the beginning of nucleation. As the growth process begins, it is characterized by a linear variation and any minute deviation in this process can be attributed to coalescence period. This region corresponds to the growth of compact inner layer. When the reaction time is increased, a sudden increase in the growth rate is observed which corresponds to the growth of a porous outer layer. The appearance of this porous layer is due to the sticking of colloids and particles from the solution. But this layer, unlike the compact layer, is weakly bonded to the substrate surface and hence can be removed easily by mechanical rubbing or sonication using ultrasonic bath.

It is considered that the governing mechanism in case of CdS is ion-by-ion process which results in the formation of adherent layers even in the presence of colloids in the solution. From this, they argue that the formation of inner compact layer should correspond to the ion-by-ion process but since there is also formation of stable colloids in the solution contributing to the compact layer growth, a combination of these two mechanisms would have to be considered. However, the

formation of porous layer indicates a structural transition and this could be attributed to the colloidal growth mechanism. This has been proved by their SEM micrographs showing large grains on the surface at long reaction times.

Based on these observations, Ortega-Borges *et al.* [18] proposed a reaction mechanism for CdS. Accordingly, the global reaction is given by:

$$Cd(NH_3)_4^{2+} + SC(NH_2)_2 + 2OH^- \longrightarrow CdS + CH_2N_2 + 4NH_3 + 2H_2O$$

By performing initial rate studies using the QCM, they arrived at the following empirical rate equation [2]:

$$r = \frac{K(T)[Cd(SO_4)]^{0.6}[SC(NH_2)_2]^{0.8}}{[NH_3]^{3.3}[H^+]^{1.5}}$$

Based on the above rate equation, they proposed the following mechanism for CdS formation [18]:

1. Reversible adsorption of cadmium hydroxide species

   $$Cd(NH_3)_4^{2+} + 2OH^- + Site \underset{k_1,k_{-1}}{\longleftrightarrow} Cd(OH)_{2ads} + 4NH_3$$

2. Formation of a surface complex with thiourea

   $$Cd(OH)_{2ads} + SC(NH_2)_2 \xrightarrow{k_2} [Cd(SC(NH_2)_2)(OH)_2]^*_{ads}$$

3. Formation of CdS with site regeneration

$$[(Cd)SC(NH_2)_2(OH)_2]^{*}_{ads} \xrightarrow{k_3} CdS + CN_2H_2 + 2H_2O + Site$$

They assumed step 3, the decomposition of metastable intermediate complex, as the rate limiting step and derived the following equation for growth rate:

$$r = \frac{k_1 k_2 [OH^-]^2 [Cd(NH_3)_4^{2+}][SC(NH_2)_2]}{k_{-1}[NH_3]^4 + k_1[OH^-]^2[Cd(NH_3)_4^{2+}] + k_2[SC(NH_2)_2] + \frac{k_1 k_2}{k_3}[OH^-]^2[Cd(NH_3)_4^{2+}][SC(NH_2)_2]}$$

Dona and Herrero [19] believed that the classical mechanism (ion-by-ion) was a homogeneous one and did not sufficiently explain the growth rate equation obtained by their analysis. Hence they did not consider it as the mechanism responsible for CBD film formation. But still, this mechanism is responsible for CdS homogeneous precipitation. Though the mechanism proposed by Lincot *et al.* deviates from their experimental rate equation, it still takes into account the heterogeneous nature of film formation and hence they believed that the deposition mechanism should be similar to the one proposed by Lincot *et al.* Hence, they proposed the next modification to this mechanism. They proposed a different intermediate species, taking into account the well-known tendency of Cd^{2+} ions to form hydroxo-ammino complexes in aqueous ammoniacal media. They arrived at the following experimental growth rate equation using initial rate studies:

$$r = \frac{K(T)[Cd(SO_4)]^{0.9}[SC(NH_2)_2]^{1.1}[OH^-]^{1.7}}{[NH_3]^{1.8}}$$

Their proposed mechanism begins with the reversible adsorption of dihydroxo-diammino-cadmium complex instead of cadmium hydroxide:

$$Cd(NH_3)_4^{2+} + 2OH^- + \text{site} \underset{k_1, k_{-1}}{\longleftrightarrow} [Cd(OH)_2(NH_3)_2]_{ads} + 2NH_3$$

Thiourea is adsorbed by this complex to form an intermediate complex according to the following equation:

$$[Cd(OH)_2(NH_3)_2]_{ads} + SC(NH_2)_2 \xrightarrow{k_2} [Cd(OH)_2(NH_3)_2\, SC(NH_2)_2]^*_{ads}$$

Finally, decomposition of intermediate complex occurs with the formation of CdS and site regeneration:

$$[Cd(OH)_2(NH_3)_2\, SC(NH_2)_2]^*_{ads} \xrightarrow{k_3} CdS + CN_3H_5 + NH_3 + 2H_2O + \text{site}$$

This reaction is considered the rate-limiting step in the mechanism. Based on this equation, they suggested the following theoretical growth rate equation for the mechanism:

$$r = \frac{k_1 k_2 [OH^-]^2 [Cd(NH_3)_4{}^{2+}][SC(NH_2)_2]}{k_{-1}[NH_3]^2 + k_1[OH^-]^2[Cd(NH_3)_4{}^{2+}] + k_2[SC(NH_2)_2] + \frac{k_1 k_2}{k_3}[OH^-]^2[Cd(NH_3)_4{}^{2+}][SC(NH_2)_2]}$$

This equation is very similar to the one derived from the mechanism proposed by Lincot *et al.*, the only difference being the exponent for the ammonia concentration, which in this modification takes a value of 2 instead of 4. The rate law can be further simplified, using the order of magnitude analysis for solution with high ammonia concentration, to get the following equation:

$$r = \frac{k_1 k_2 [CdSO_4][SC(NH_2)_2][OH^-]^2}{k_{-1}[NH_3]^2}$$

This equation is very similar to the experimental one, which supports their theoretical mechanism.

For a long time, CBD was not studied from an engineering point of view by researchers who mainly focused on deposition process, film characterizations and mechanisms involved. It was Nair *et al.* [20] who first attempted to model the CBD process describing the growth mechanism of thin films produced by a batch process. They identified three different stages in the CBD growth process *viz.* nucleation phase, growth phase and a terminal phase. Each of these phases depends on various factors such as concentration of ions in the bath, the deposition temperature and dissociation constants of metal ions. They showed that the

proposed mathematical model, with the assumption of first order kinetics, was in good agreement with their experimental conditions.

Later, Kostoglou *et al.* [21] did an extensive mathematical modeling of CBD process by considering the rates for each phenomena involved *viz.* particle nucleation, growth, coagulation and deposition. The nucleation was modeled based on the classical theory of nucleation as:

$$\alpha = \frac{1}{6}\pi\left(\frac{4V_m\sigma}{nRT\ln(s)}\right)^3$$

where α is the volume of the nucleus, V_m the molecular volume of CdS, R the ideal gas constant, T the temperature, S the supersaturation and σ the interfacial tension.

Here the modeling takes into account the dependence of critical size on supersaturation. Their simplified model is based on the assumption that there will be instantaneous nucleation and growth phenomena (instead of the continuous one) at supersaturation point. This in turn means that during the period before supersaturation is achieved, there would be no particle formation and the film growth becomes slow and stops eventually when supersaturation is reached. There was a good agreement between the experimental data and the values from the simplified model. They also modeled particle deposition as:

$$D(x) = \frac{0.3D_p^{2/3}u_\infty^{1/2}}{W_d v^{1/6}L^{1/2}}$$

where D(x) is the diffusivity of particles of volume x, v the kinematic viscosity of the solution, u a characteristic velocity of the fluid, L the characteristic length of the submerged surface and W_d the stability ratio for particulate deposition. They performed a comprehensive model analysis and their preliminary calculations indicated that the final thickness of film due to particle deposition was twice the thickness contributed by heterogeneous reaction for the unit value of W_d.

More recently, Voss *et al.* [22] monitored CBD CdS growth kinetics using QCM. They observed that the film growth could be limited at certain concentrations and temperatures and that it is strongly dependent on the stirring rate. They identified four distinct growth regimes. A slow induction regime was followed by linear compact growth which transformed into a porous layer growth marked by a "kink" in the growth curve. The final phase, the depletion regime, was a result of the depletion of the reactants and thus the film growth slowed down and eventually stopped. They also observed that the dramatic change in the concentration of Cd during linear compact growth regime had no effect on the deposition rate which remained constant during the regime. They concluded that the growth of CBD films could be due to a combination of molecule-by-molecule (ion-by-ion) and cluster-by-cluster mechanism.

Based on these extensive reviews of growth mechanisms proposed by various research groups, our current understanding [18,21] of CBD CdS mechanism can be best illustrated using the schematic diagram as given in fig 4.1 [1].

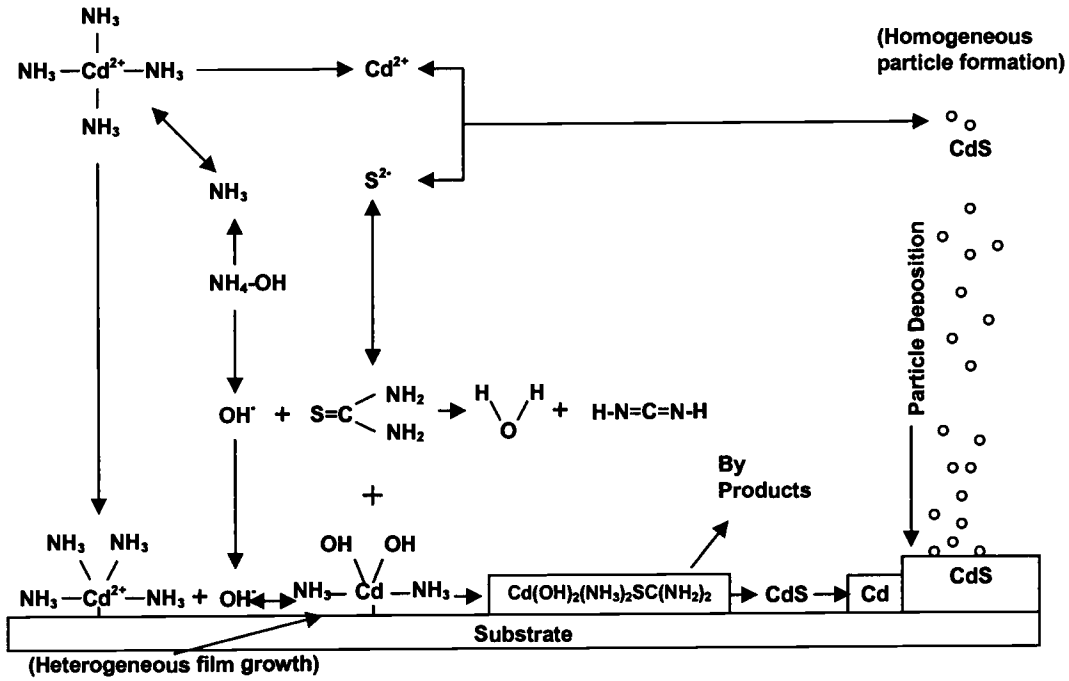

Figure 4.1 Schematic of CBD CdS growth process

Although there are many independent chemical reactions occurring in the solution bath, they could be classified into two major categories as homogeneous particle formation (precipitation) and heterogeneous film growth (surface reaction) [19]. In the bulk of the alkaline solution, ammonium hydroxide provides ammonia which complexes with free Cd^{2+} ions released by the decomposition of a cadmium salt (such as $CdCl_2$) to form tetramino-cadmium complex ion $Cd(NH_3)_4^{2+}$. Thiourea undergoes slow hydrolysis in the basic solution releasing free S^{2-} ions. Free Cd^{2+} and free S^{2-} ions react to form CdS particles which precipitate in the solution bath. The surface reaction involves the tetramino-cadmium complex and hydroxide ions to form dihydroxo-diamino-cadmium complex. Thiourea is

adsorbed by this complex to form an intermediate complex $[Cd(OH)_2(NH_3)_2 SC(NH_2)_2]^*_{ads}$. Finally, this adsorbed intermediate complex undergoes decomposition to produce CdS.

Through our studies involving batch CBD process, we tried to further improve upon our current understanding of CBD CdS mechanism. Figure 4.2 shows the growth kinetics studies made by QCM. It indicates that the film growth started in the linear growth regime, through ion-by-ion process, and quickly changed to the porous growth regime (after 100 s) which is through particle sticking mechanism.

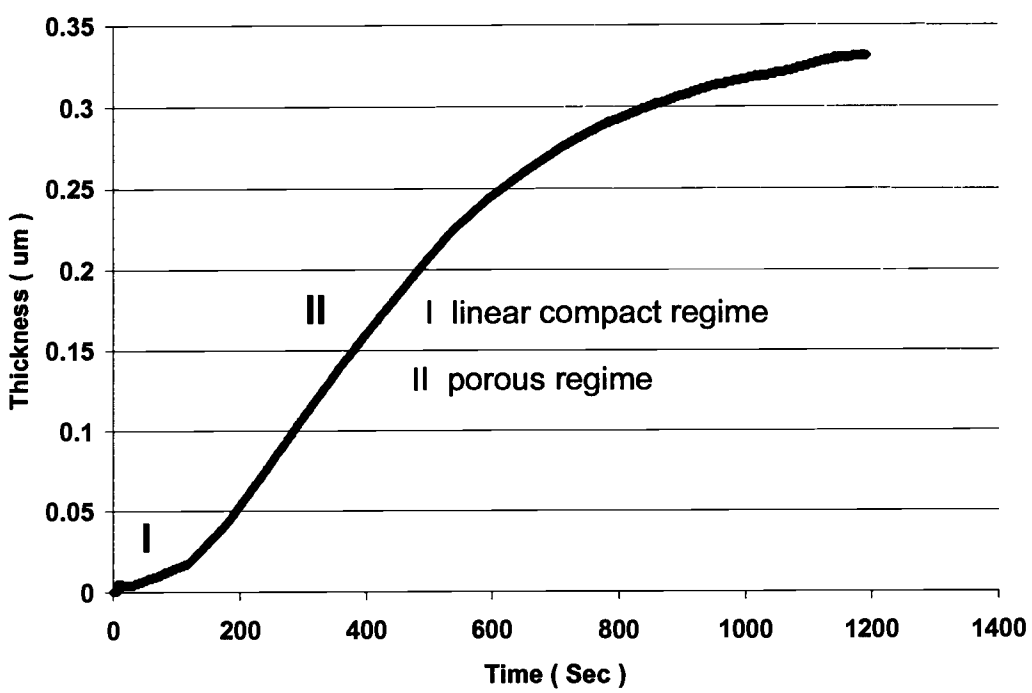

Figure 4.2 QCM growth curve for batch CBD process

Figure 4.3 shows a corresponding SEM image of CdS film with a deposition time of 8.5 mins.

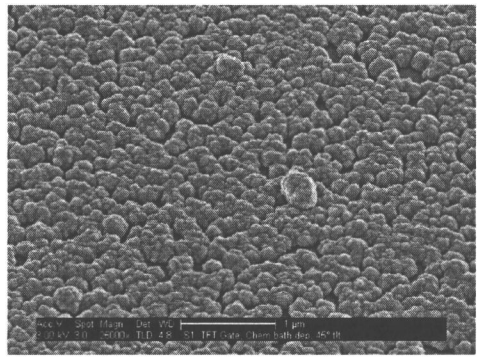

Figure 4.3 SEM image of CdS film by batch process (t = 8.5 mins)

Both QCM and SEM analysis indicate that the film growth during the linear compact regime was short as compared to the predominantly longer porous growth regime. From this we can conclude that the growth of these CBD CdS films is well dominated by the particle sticking mechanism.

To further confirm the homogeneous particle formation, AFM analysis was done. Figure 4.4 shows the AFM images of CBD solution taken at 5 and 10 min intervals during the batch process. As seen in figure 4.4 (a), the presence of a number of rod shaped particles along with smaller round shaped particles could be due to crystallization of unreacted thiourea during the process. But 10 min after the reaction, as seen in figure 4.4 (b), these rod shaped particles could not be seen and instead they are replaced by a large number of round shaped particles which are presumably CdS particles.

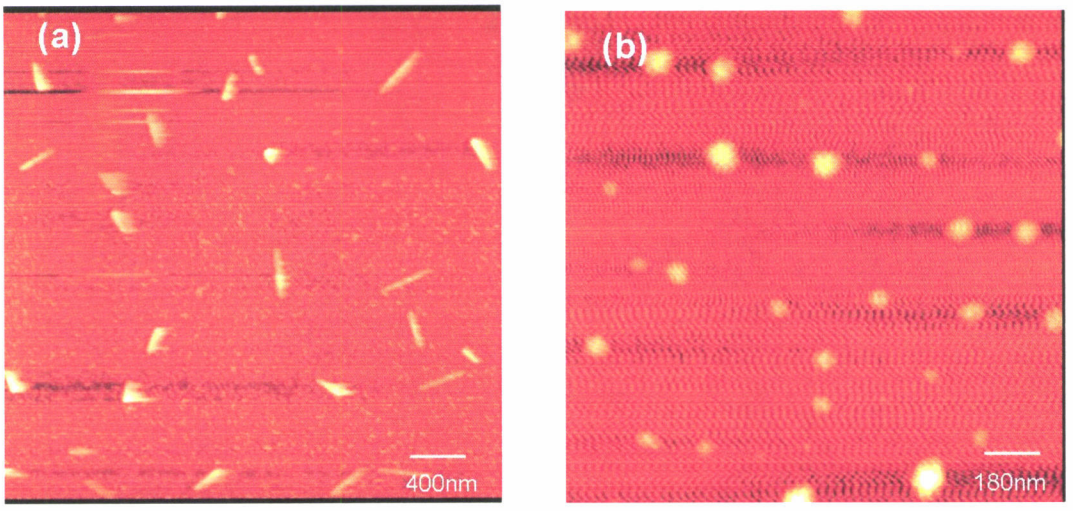

Figure 4.4 AFM images of CdS particles (a) 5 min and (b) 10min after reaction

This clearly shows that the round shaped CdS particles were growing in the solution bath even during the initial stages of the reaction by consuming sulfur from thiourea. Comparing with our QCM curve, the reaction times (5 and 10 min) are well within the porous growth regime thus confirming the dominating homogeneous particle formation mechanism.

So far the discussion has been confined to batch CBD process. In case of continuous flow microreactor, the deposition process can be controlled. Though there is no chemical bath involved as such, still the homogeneous precipitation can occur if the residence time of the impinging solution inside the coil is long enough. Accordingly, it could be a combination of both homogeneous precipitation and heterogeneous deposition. But in our present study, the residence time was short

enough to prevent homogeneous precipitation inside the coil. Hence the impinging solution was particle free. This has been confirmed from our UV-Visible absorption measurements carried out on product solution from the microreactor setup. There was no indication of any absorption spectrum when measurements were made using DI water as background solution. However, when thiourea was used as background solution, a typical absorbance was observed which was later attributed to the characteristic absorbance spectrum of thiourea. Our observations were also confirmed by TEM measurements (see TEM discussion under section 4.3).

Since it is a continuous process, the fresh reactants are mixed continuously in micromixer and the resulting product solution will impinge on the hot substrate maintained around 80-90°C. The reaction takes place on the surface of the substrate where the heat from the substrate provides the energy needed for reaction resulting in heterogeneous deposition. On the contrary, in case of batch process, the heat required for chemical reaction is delivered from the solution bath to the sample surface resulting in both heterogeneous nucleation at the surface and homogeneous CdS formation in the bath.

Thus, from our current understanding of CBD process, we can summarize our discussion in the following manner:

- In case of batch CBD, film formation could be due to a combination of both homogeneous particle formation (cluster-by-cluster growth) and heterogeneous deposition (molecule-by-molecule growth).
- In case of continuous flow microreactor setup, the mechanism of film formation can be controlled based on the residence time distribution of the impinging solution. In our case, the film formation was only by heterogeneous deposition.

4.3 Characterizations of CdS thin films

The CdS thin films produced by batch and continuous flow microreactor setup were characterized by XRD, XPS and TEM to determine the various structural and chemical properties.

XRD

A thin film (about 500 A) of CdS was deposited on silicon coupon using the CFM and microstructurally characterized by X-ray diffractogram (XRD). Due to its limited thickness, no diffraction peak was shown by XRD except the peak for the SiO_2 substrate. Figure 4.5 shows the typical diffractogram obtained for CdS film of thickness around 2500 A. Since the thickness is limited by the syringe pump capacity (50 ml.), the deposition had to be done for four times on the same coupon, in order to grow a thick film, at a temperature of 85-90 ^{o}C.

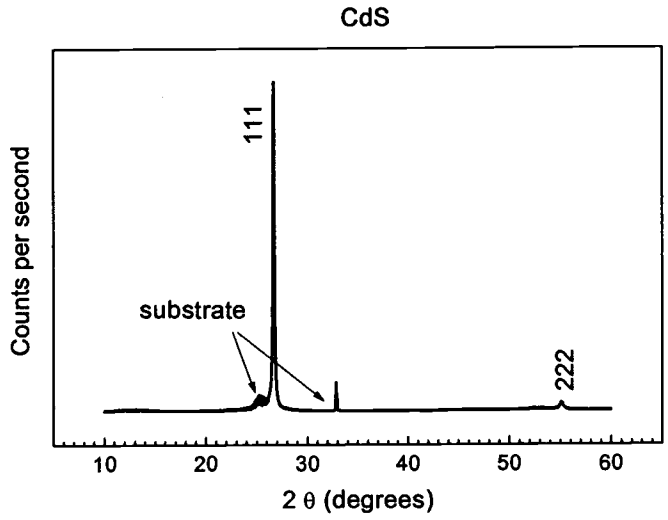

Figure 4.5 X-ray diffractogram of CdS film

The graph shows diffraction peaks at $2\theta = 26.5^{\circ}$ and $2\theta = 55^{\circ}$. These diffractogram peaks were compared with the standards in the JCPDS data files (card number 80-0019, 75-0581, 42-1411, 75-1546). The as-deposited material appears to be composed of the cubic phase of CdS although the possibility of the hexagonal phase can not be ruled out. The sharp peak at 26.5° corresponds to the (111) Bragg reflection planes from the cubic (zincblende) phase and the graph clearly shows that the film is strongly oriented along (111) with another small orientation at (222). For testing the accuracy of our result and for comparison, XRD was also done for bare silicon coupon and the peaks obtained are shown in the same graph. For all practical purposes, we can only consider the orientation at (111) since it is very strong compared to the other one. Thus, the presence of only

one peak indicates the highly oriented nature of CdS films, which must grow as successive alternative planes composed of only Cd or S atoms parallel to the substrate surface, as it corresponds to the (111) planes of the cubic crystalline structure. This type of growth is in good agreement with the modified mechanism of CBD proposed by Dona *et al* [19] based on the adsorption of the dihydroxo-diammino-cadmium complex and the successive formation of the metastable complex by the adsorption of a thiourea molecule on the adsorbed cadmium complex.

CdS can exist in three different crystal forms: hexagonal (wurtzite), cubic (zincblende or sphalerite) and cubic (rocksalt). Except in a few cases, the rocksalt form of CdS has been observed only at very high pressures and CBD films of this form have never been reported. The other two forms have been reported to occur in CBD films under different conditions. The hexagonal form is thermodynamically more stable and usually occurs if the zincblende phase is heated above 300-400°C [25].

XPS

The CdS layers deposited by batch and CFM were analyzed by XPS. The XPS spectra for our CBD CdS were typical for CdS films reported by other researchers [29, 30].The binding energies of Cd $3d_{5/2}$ and Cd $3d_{3/2}$ at ~405.2eV and ~411.9 eV and that of S 2p at ~161.5 eV for the films were indicative of the CdS chemistry. An important observation was the presence of carbon and oxygen as

impurities in the as-deposited and annealed films (Table 4.1, 4.2). The carbon peak, present in these samples, was of little informational utility since it is present as an impurity in all the samples exposed to atmosphere and analyzed by XPS [14].The energy scale was calibrated using this carbon peak (C 1s at 284.8 eV) as a reference. The O 1s line possesses a rather narrow bandwidth and symmetric shape and is an indication of the presence of some oxidation products on the surface of the film.

After annealing, a concentration of chloride species was observed in the XPS spectrum of microreactor produced CdS film. Similar observations were made by other group of researchers employing the SIMS technique [31] and XPS [32]. The chlorine concentration in annealed film could be attributed to the reagents $CdCl_2$ and/or NH_4Cl used for the preparation of CdS layers by CBD and the Cl 2p peak position at ~199 eV corresponds to Cl bonded as $CdCl_2$ [33]. The Si 2p peak in the batch produced (annealed) film at binding energy of 103.2 eV suggests SiO_2 and is more likely due to the presence of pinholes in the film. The figures from 4.6 to 4.19 show a comparative study of XPS spectra of various elements for both batch and continuous microreactor produced films, as-deposited and after annealing.

Table 4.1 XPS data for as-deposited CdS films and associated Binding Energy (eV) peaks (in good agreement with literature values [35, 36]).

Photoelectron peak	**Binding energy (eV)**		
	Batch	**CFM**	**Lit. Values**
Cd $3d_{5/2}$	405.2	405.1	405.2
Cd $3d_{3/2}$	411.9	411.7	411.9
S 2p	161.7	161.4	162.5
O 1s	532	531.6	543.1
C 1s	284.7	284.6	284.2

Table 4.2 XPS data for annealed CdS films and associated Binding Energy (eV) peaks (in good agreement with literature values [35, 36]).

Photoelectron peak	**Binding energy (eV)**		
	Batch	**CFM**	**Lit. values**
Cd $3d_{5/2}$	405.2	405.4	405.2
Cd $3d_{3/2}$	411.9	412.1	411.9
S 2p	-	161.5	162.5
O 1s	532.5	531.7	543.1
C 1s	284.7	284.7	284.2
Si 2p	103.2	-	99.8
Cl 2p	-	198.7	200

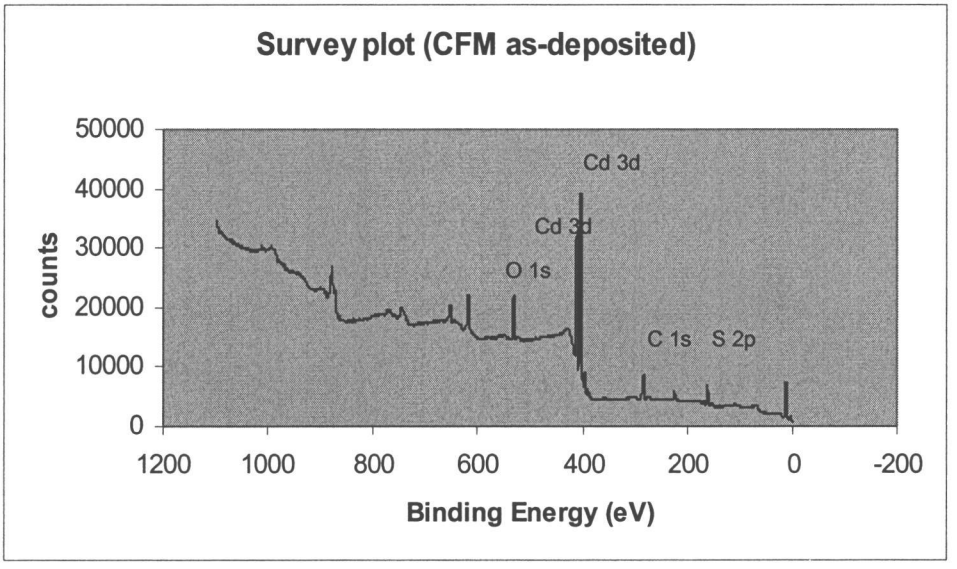

Figure 4.6 Survey plot of CFM film without annealing

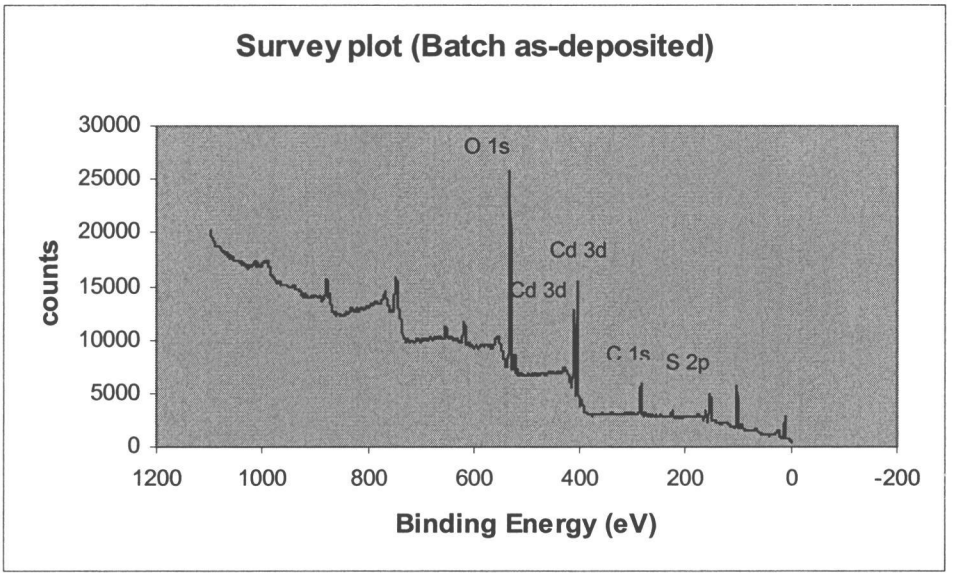

Figure 4.7 Survey plot of batch film without annealing

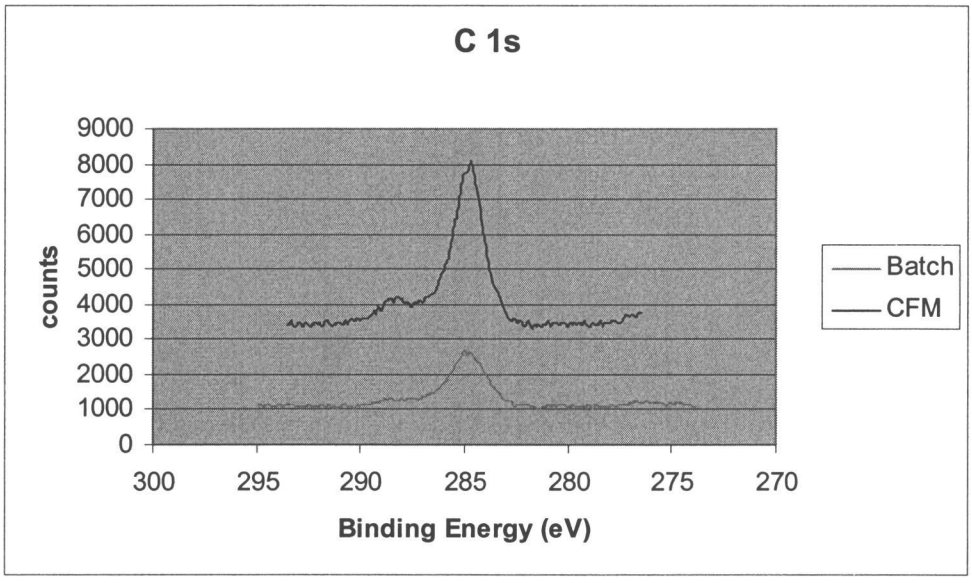

Figure 4.8 C 1s spectrum of CdS films without annealing

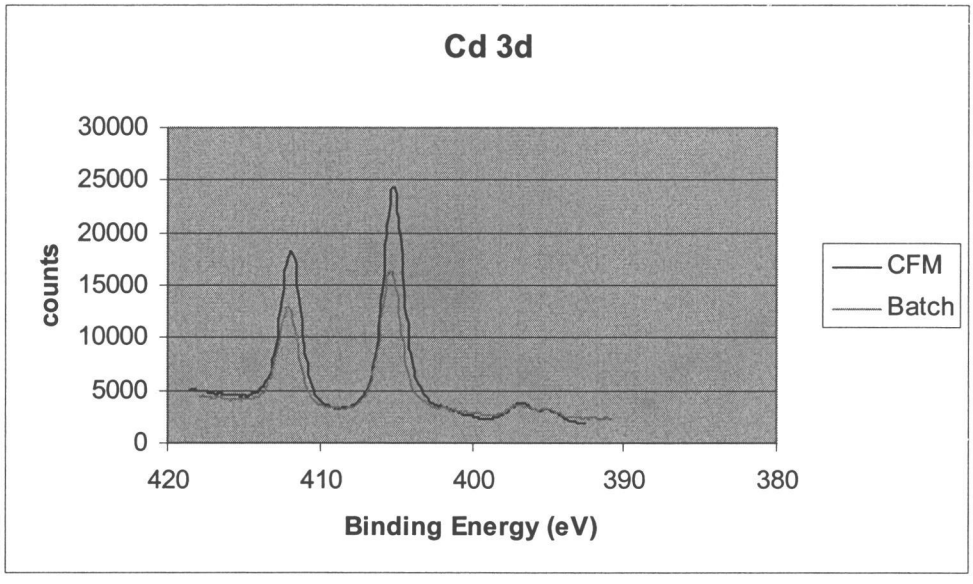

Figure 4.9 Cd 3d spectrum of CdS films without annealing

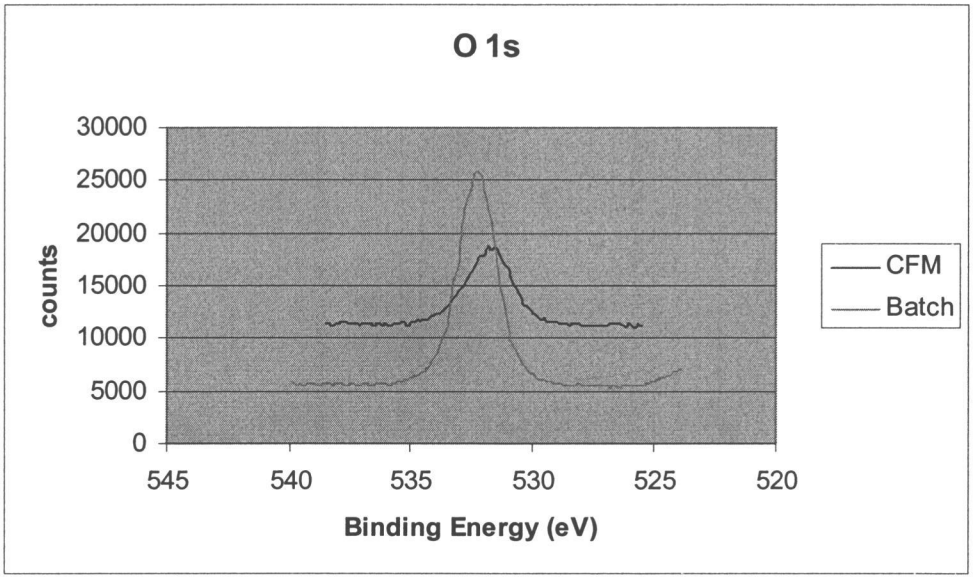

Figure 4.10 O 1s spectrum of CdS films without annealing

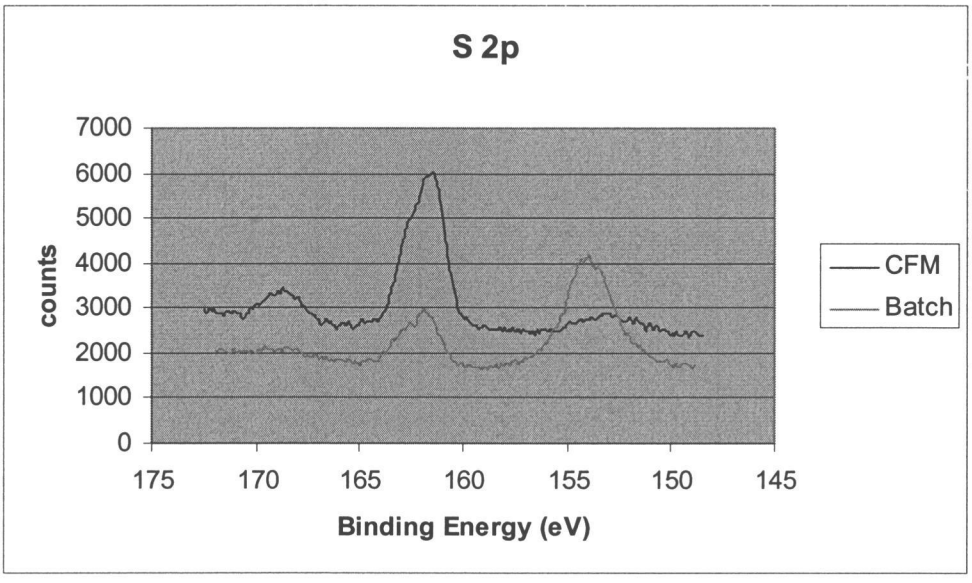

Figure 4.11 S 2p spectrum of CdS films without annealing

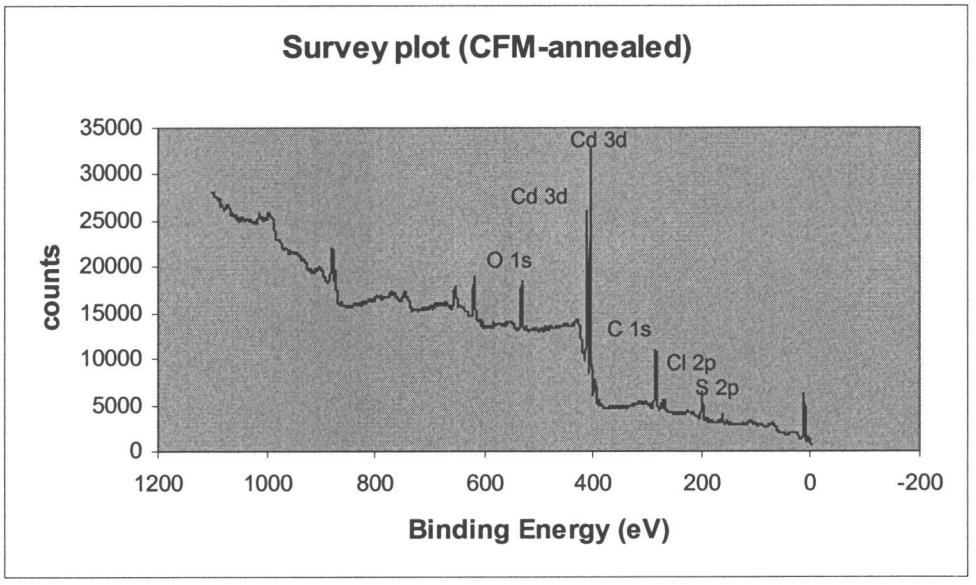

Figure 4.12 Survey plot of CFM film after annealing

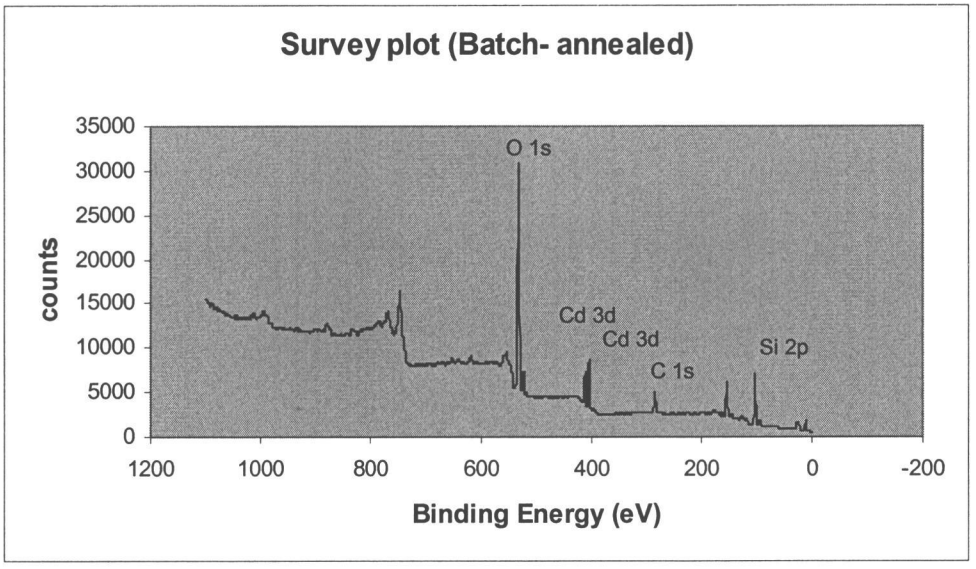

Figure 4.13 Survey plot of batch film after annealing

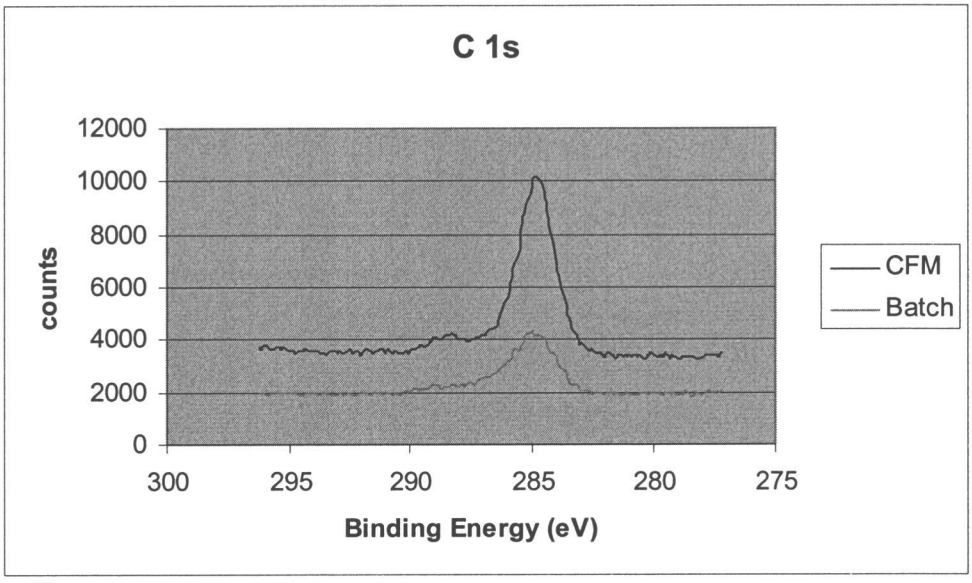

Figure 4.14 C 1s spectrum of CdS films after annealing

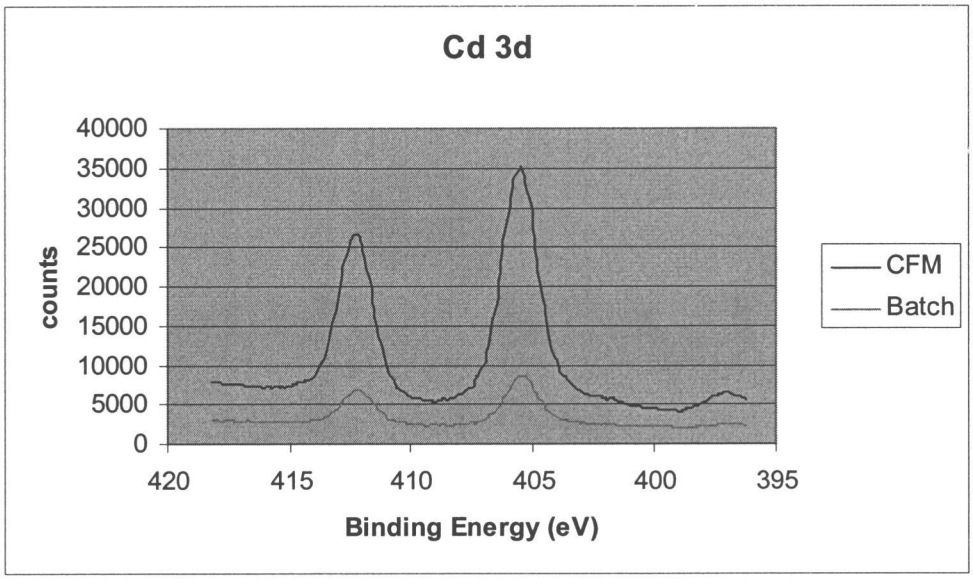

Figure 4.15 Cd 3d spectrum of CdS films after annealing

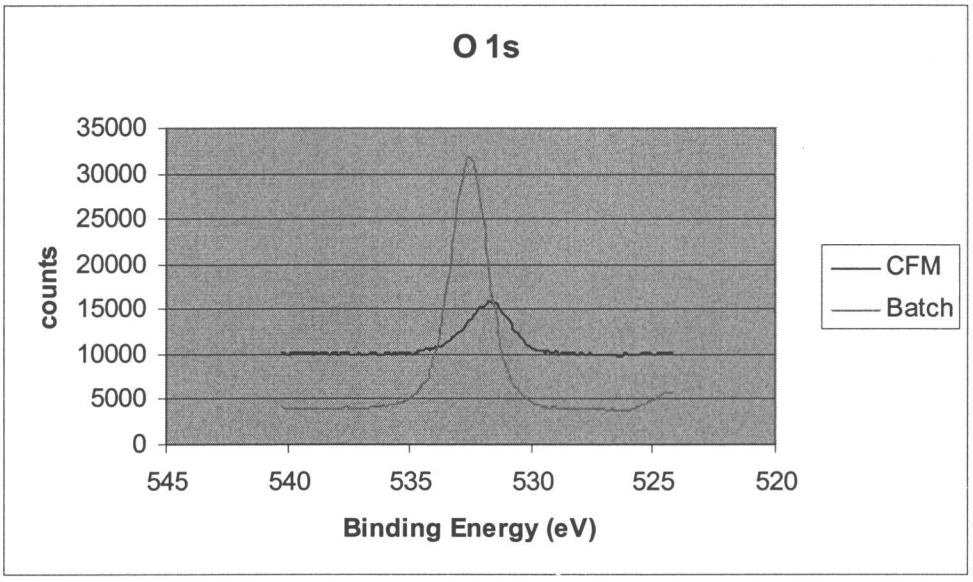

Figure 4.16 O 1s spectrum of CdS films after annealing

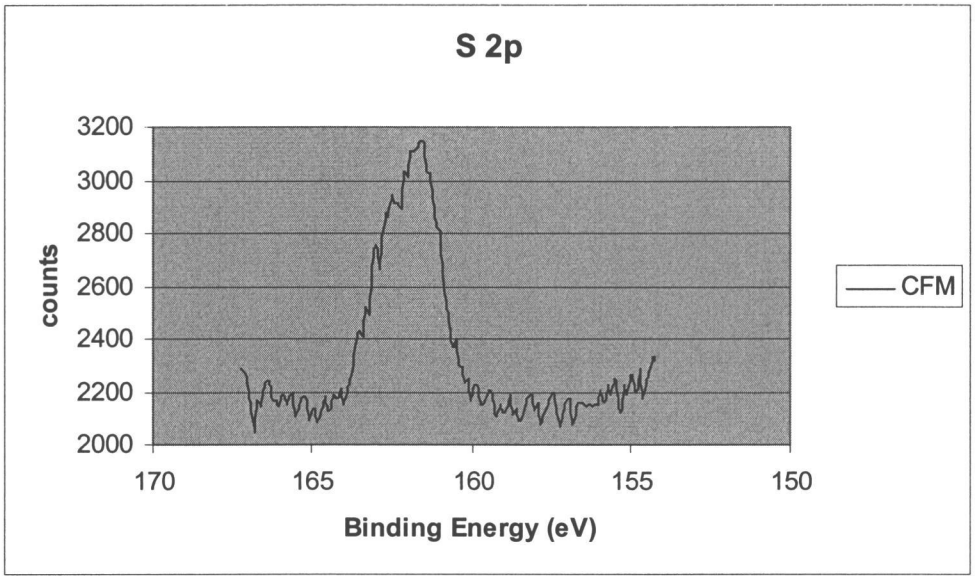

Figure 4.17 S 2p spectrum of CdS films after annealing

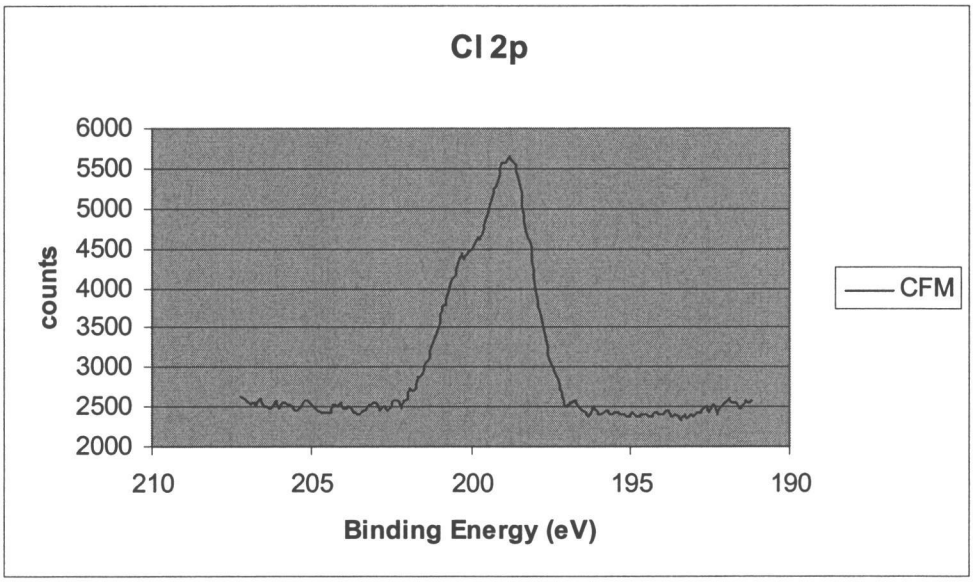

Figure 4.18 Cl 2p spectrum of CdS films after annealing

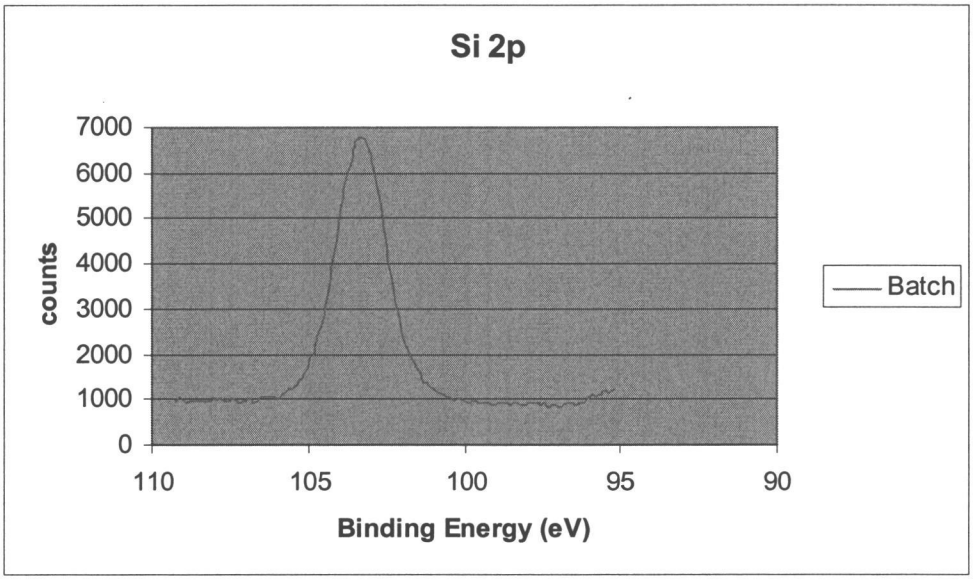

Figure 4.19 Si 2p spectrum of CdS films after annealing

TEM

With the objective of developing the CdS film microstructure, we prepared CdS deposits on copper grids covered by thin lacey carbon films to be studied by TEM, SAED and EDX. Figure 4.20 shows the TEM micrographs of CdS particles obtained by dipping the grid, for 10 sec, in batch reactor solution at 80°C when the reaction time t was 3.12 min.

We can see many agglomerates like bunch of grapes with particles over 0.1 μ m in size as in (a). Each of these particles in turn contains a mixture of crystalline grains (b) of the order of 10 nm in diameter.

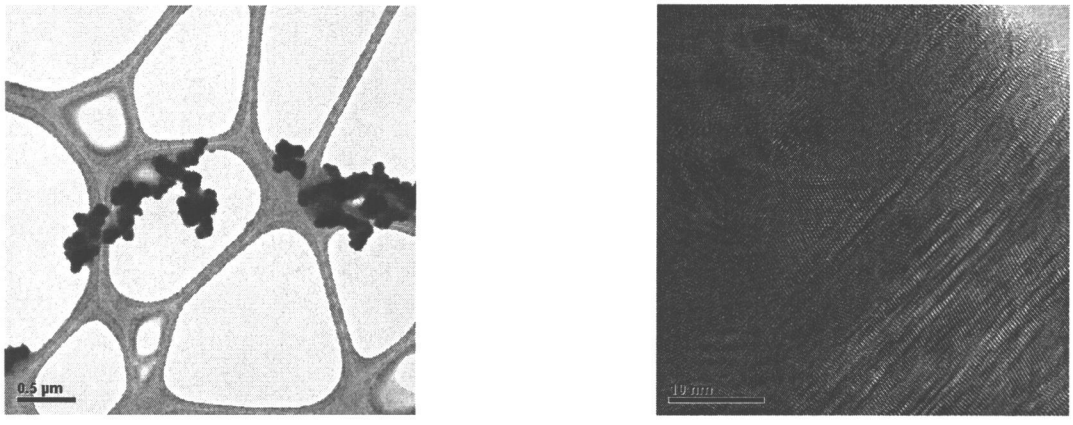

(a) **(b)**

Figure 4.20 TEM micrographs of CdS particles produced from batch reactor

The SAED pattern, as given in figure 4.21, shows more spots as expected from the slightly larger grain size. The observed lattice plane spacing (d) values

are in good agreement with the JCPDS power diffraction data for the cubic phase of CdS as shown in the same figure. Also, the experimental lattice constant a = 5.87 A is in good agreement with the literature value of 5.82 A for cubic CdS phase.

In the EDX spectrum, as in figure 4.22, the peaks of Cd and S are pronounced with Cd/S ratio of 43.1/56.9 atomic %. The presence of Cl peak may be due to the reagents $CdCl_2$ or NH_4Cl used in the CBD process and Cu peak can be attributed to copper grids used in the sample preparation process.

Observed d-spacing values (A)	JCPDS 80-0019 (Cubic CdS)
3.36	3.35 (111)
	2.91 (200)
2.07	2.05 (220)
1.77	1.75 (113)
	1.68 (222)
	1.45 (400)
1.35	1.33 (331)
	1.29 (420)

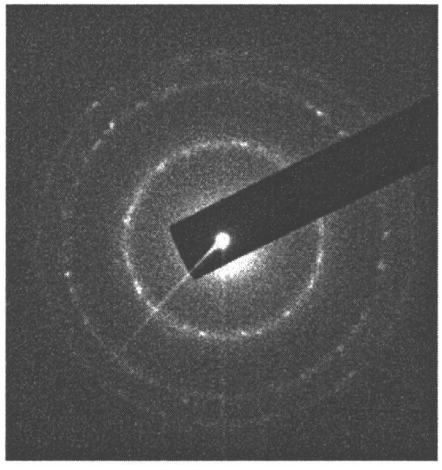

Figure 4.21 SAED pattern of CdS (batch reactor)

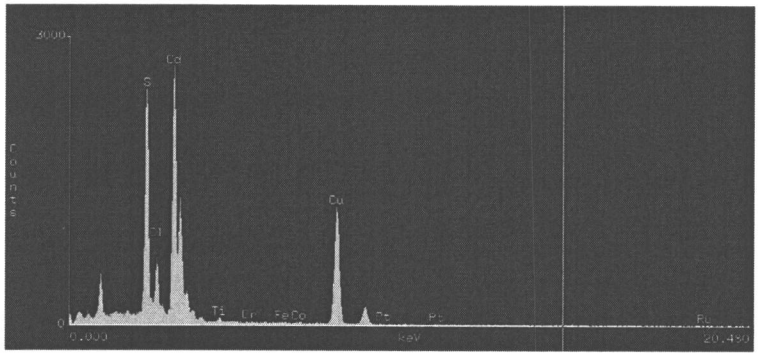

Figure 4.22 EDX spectrum of CdS (batch reactor)

A comparative study was made by depositing CdS film on copper grids covered with thin lacey carbon films using CFM and the same was analyzed by TEM and other techniques. Figure 4.23 shows TEM micrographs of CdS film deposited using CFM at 80°C with a deposition time of 3.12 min.

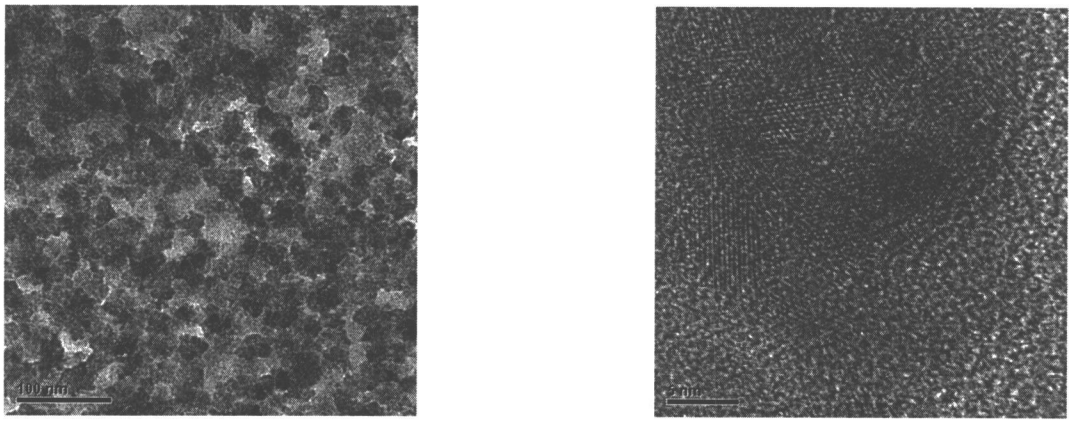

(a) **(b)**

Figure 4.23 TEM micrographs of CdS film produced by CFM

We can observe the distribution of small grain agglomerates and individual grains reach up to 5 nm in diameter as shown in (a) and (b). These particles must be the origin of the film after coalescence. The corresponding SAED diagram, as shown in figure 4.24, indicates the formation of a polycrystalline film and is composed of well defined rings but the first ring is diffuse possibly originating from the samples with poor crystallinity. It can be seen that the measured d-spacing values are in good agreement with the hexagonal CdS phase. Also, the experimental lattice parameters of a = 4.09 A and c = 6.77 A were reported, in good agreement with the literature values of 4.13 A and 6.75 A respectively.

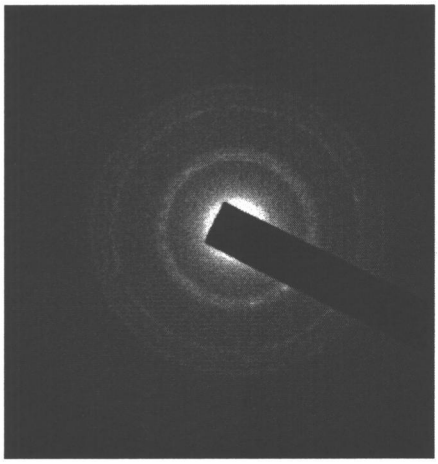

Observed d-spacing values (A)	JCPDS 80-0006 (Hexagonal CdS)
3.54	3.57 (100)
3.39	3.34 (002)
3.25	3.15 (101)
2.51	2.44 (102)
2.08	2.06 (110)
1.94	1.89 (103)
1.79	1.78 (200)

Figure 4.24 SAED pattern of CdS film (CFM)

The EDX spectrum for this film is given in figure 4.25. It shows a Cd to S ratio of 42.3/57.7 atomic %. Again, Cu peak can be attributed to copper grids used in the sample preparation process.

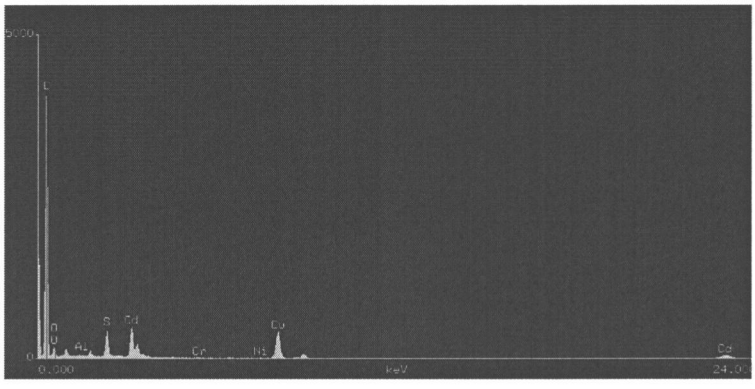

Figure 4.25 EDX spectrum of CdS film (CFM)

Also, TEM measurement was done by dipping copper grid (with thin lacey carbon film) in hot solution, collected from CFM, for about 10 sec and observing through the microscope. There was no evidence of any particles on the surface of the grid as shown in figure 4.26. This sample had no crystallinity and nothing of interest was found. Also, the EDX did not show any CdS.

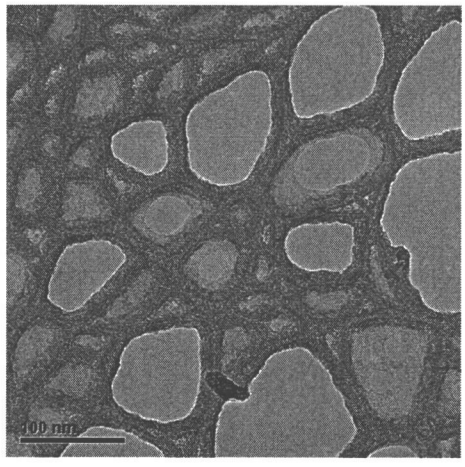

Figure 4.26 TEM image showing absence of CdS particles from CFM solution

4.4 Morphology of CdS thin films

The film morphology was investigated using AFM, Profilometer and SEM analysis techniques. Figure 4.27 compares 2 μm x 2 μm AFM scans of CBD CdS films deposited on silicon wafer coupons using batch and CFM processes.

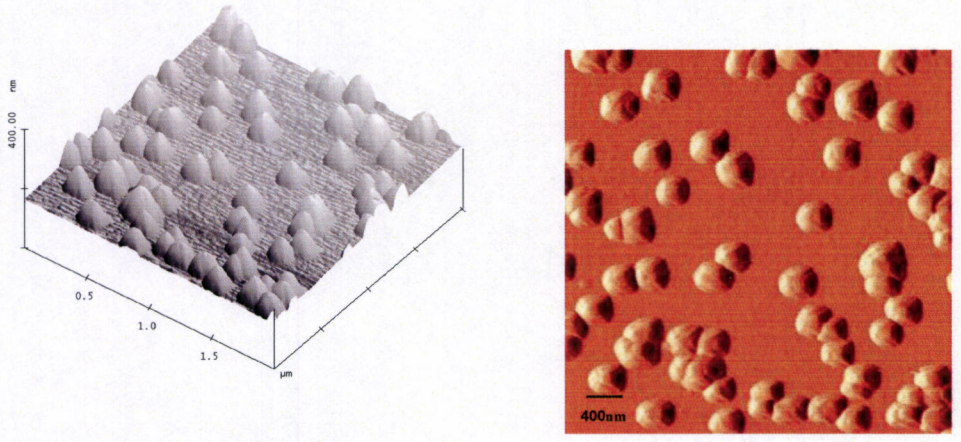

(a)

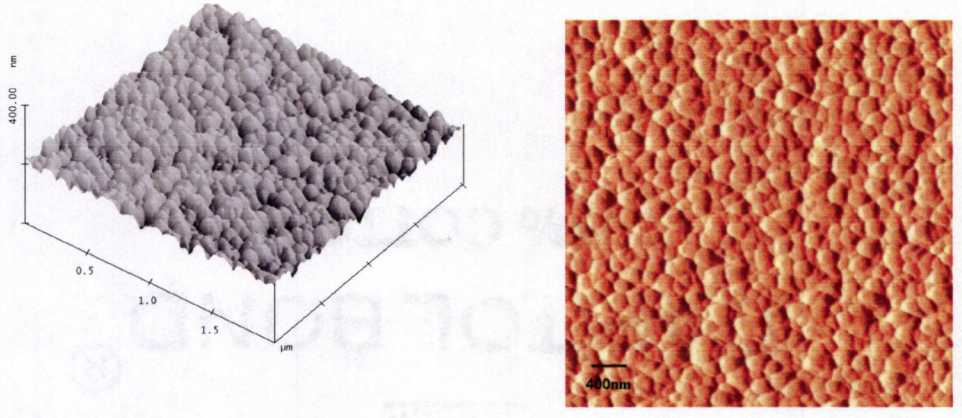

(b)

Figure 4.27 AFM images of CdS films deposited by (a) batch and (b) CFM

These AFM images reveal clear differences in the appearance of the surface for samples deposited by batch and CFM. Fig 4.27 (a) shows the surface morphology of batch deposited film having root mean square (RMS) surface roughness of 19.592 nm with a mean roughness of 15.795 nm. The grains appear

to be big and dispersed all over the surface. Fig 4.27 (b) shows the surface morphology of CFM deposited film of the same scan size (2μm x 2μm). The RMS value of roughness was found to be 11.751 nm with a mean roughness of 9.606 nm which indicates that the film is much smoother than the batch deposited film. We can clearly see that the grains are smaller (compared to batch) and more evenly dispersed on the surface indicating that the films are more uniform than those produced by batch process. Some two-dimensional images of different scan sizes are included in Appendix B.

The differences in the appearance of surface topography were further confirmed with the help of profilometer (Dektak) as shown in figure 4.28 (a) and (b). As seen clearly, the CFM deposited film has fewer peaks and hence is much smoother than the batch deposited film.

(a)

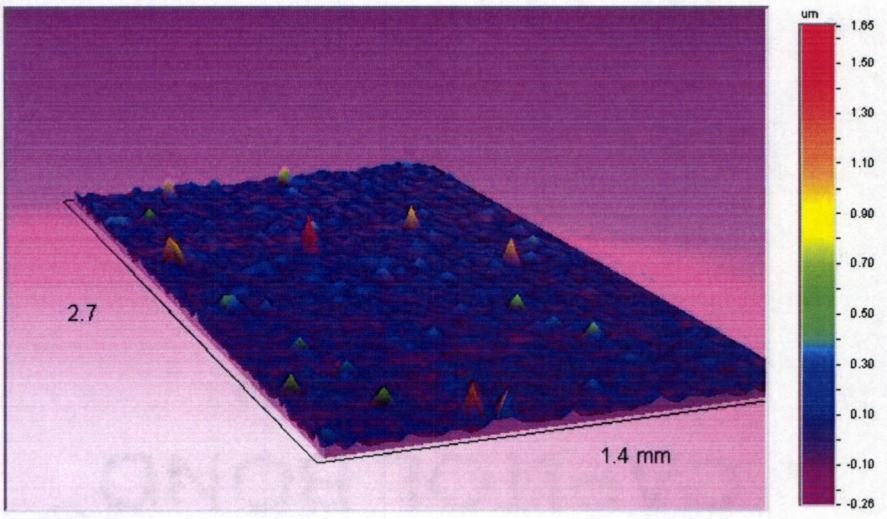

(b)

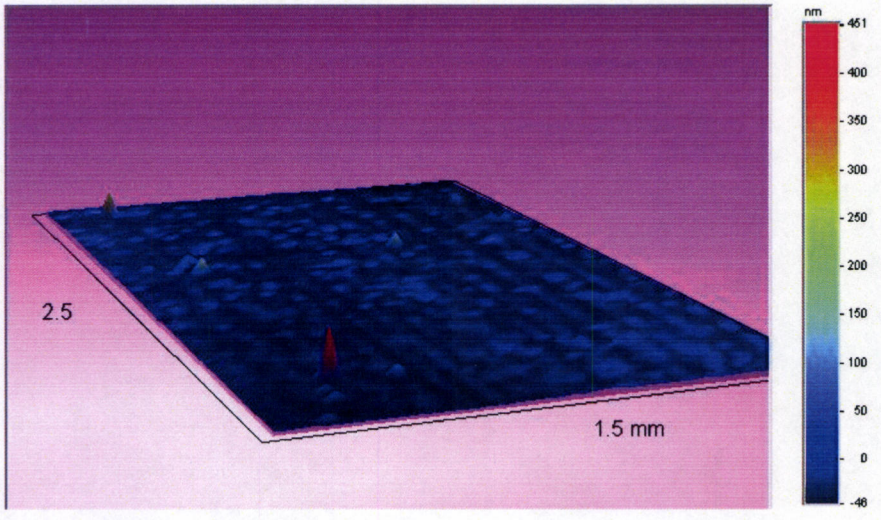

Figure 4.28 Profiler images of CdS films deposited by (a) batch and (b) CFM

Figure 4.29 shows top-view SEM images of CdS film deposited by batch and CFM.

(a)

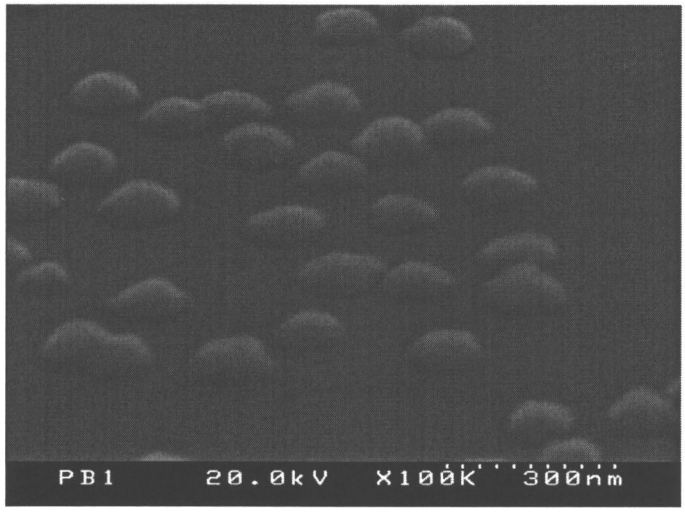

(b)

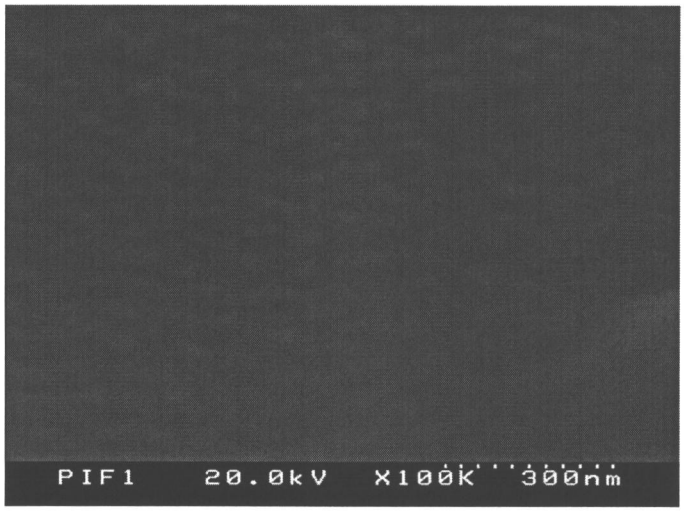

Figure 4.29 Top view images of CdS film by (a) batch and (b) CFM

As seen in (a), the average grain size of particles is approximately 150 nm for a film whose thickness is approximately 100 nm. Particles are dispersed unevenly in few numbers and large sizes. On the contrary, the particles are distributed more uniformly in large numbers and small sizes for the film produced by CFM as shown in (b). The average grain size is approximately 70 nm with a film thickness of approximately 50 nm.

CHAPTER 5

CONCLUSIONS AND FUTURE WORK

6.1 Conclusions

In this work, a novel continuous flow microreactor has been developed based on the chemical bath deposition process. Films of CdS were deposited by conventional batch CBD reactor from heated solutions and also by CFM with heated substrates. Various characterization results showed that CFM deposited films were more uniform and of better quality than the batch deposited ones.

Our newly developed CFM works on the principle of 'heterogeneous deposition' wherein the heat from the substrate and the impinging solution provides the energy needed for surface reaction. In this way, unwanted deposition on the walls of the vessels and the homogeneous CdS formation in the chemical bath is avoided. Mixing is achieved with the help of micromixer which is far more superior than the conventional agitation equipment used in batch processes. Furthermore, the continuous process has resulted in minimization of waste production leading to more uniform films with negligible occurrence of pinholes.

6.2 Future work

The CFM developed in the course of this study could be considered as an initial design which needs further modifications in order to be able to consistently produce high quality films by the CBD process. The major challenge is the control

of fluid flow and uniform distribution of flow over the entire heated surface of the substrate. One of the proposed designs of the hot plate surface is given in figure 6.1 in which the silicon substrate is taped on to a metallic disc and then a transparent plexi glass plate, with provision for inserting tube, is used to cover the disc so that the solution can flow perpendicular to the surface of the substrate and distributed uniformly across the surface. This type of arrangement would result in a more even distribution of the impinging hot solution and produce more uniform films.

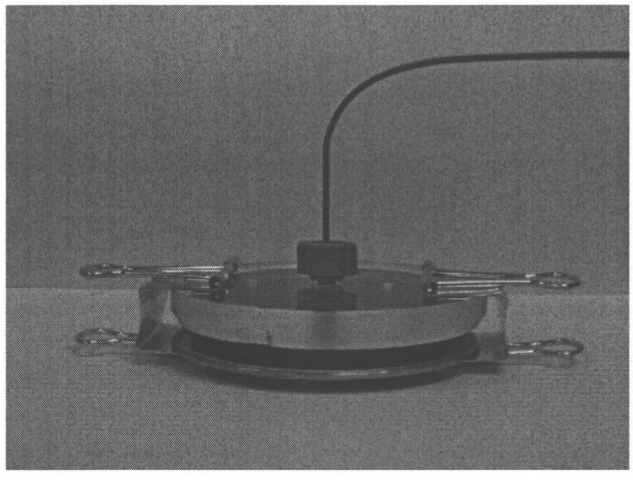

Figure 5.1 Modified design for CFM cover plate

Secondly, the films produced using CFM could be used for fabricating thin film transistors (TFTs) and other flexible semiconductor devices. Indeed, the I-V characterizations showed an enhanced mode transistor behavior in our first attempt

to make a device using CdS thin films deposited by CFM (without any post annealing treatment).

Our discussion in this study has been limited to only CdS but it is worth noting that cadmium is a carcinogenic agent and one of the most dangerous elements which pose serious threat to the environment. For this reason, other environmentally benign materials will be chosen for fabricating devices. A host of other semiconductors such as CuS, ZnO, ZnS, ZnSe, CuO could be deposited using the new reactor. However, the recipe for each material as well as the process conditions needs further investigation.

Lastly, the same reactor could be used for studying the particle growth kinetics. The inclusion of a quasi elastic light scattering (QELS) system in the CFM setup will enable the *in-situ* monitoring of particle sizes and their distributions.

BIBLIOGRAPHY

1. Y.-J.Chang, C.L.Munsee, G.S.Herman, J.F.Wager, P.Mugdur, D.-H.Lee, C.-H. Chang, submitted to *Surface and Interface Analysis* (2004).
2. R.Ortega-Borges, M.Froment, J.Vedel, D.Lincot, *Solid State Phenom.*, 37-38, 497 (1994).
3. P.K.Nair, V.M.Garcia, O.Gomez-Daza, M.T.S.Nair, *Semicond.Sci.Technol.* 16 (2001) 855-863.
4. J.E.Reynolds, *J.Chem.Soc.*45, 162 (1884).
5. "*Physics of Thin Films*", D.E.Bode, 3, 275 (1966).
6. J.Bloem, *Appl.Sci.Res.*B 6, 92 (1956).
7. G.A.Kitaev, A.A.Uritskarya, S.G.Morkrushin, *Russ.J.Phys.Chem.*, 39, 1101 (1965).
8. R.A.Zingaro, D.O.Skovlin, *J.Electrochem.Soc.*, 11, 42 (1964).
9. G.A.Kitaev, S.G.Mokrushin,A.A.Uritskaya, *Colloid J.USSR*, 27,38 (1965).
10. M.J.Mangalam,, K.N.Rao, N.Rangarajan, C.V.Suryanarayana, *Brit.J.Appl.Phys.*2,2,1643 (1969).
11. K.L.Chopra, R.C.Kainthla, D.K.Pandya, A.P.Thakoor, *Phys.Thin Films* 12,167 (1982).
12. K.Vaccaro, H.M.Dauplaise, A.Davis, S.M.Spaziani, J.P.Lorenzo, *Appl.Phys.Lett.*, 67, 527 (1995).

13. I.Kaur, D.K.Pandya, K.L.Chopra, *J.Electrochem.Soc.*, 127, 943 (1980)

14. P.C.Rieke, S.B.Bentjen, *Chem Mater.*, 5, 43 (1993).

15. D.Lincot, R.Ortega-Borges, *J.Electrochem.Soc.*, 139, 1880 (1992).

16. G.A.Kitaev, Y.N.Makurin, V.I.Dvoinin, *Russ.J.Phys.Chem.*, 50, 1828 (1976).

17. N.D.Betenekov, V.P.Medvedev, G.A.Kitaev, *Sov.Radiochem.*, 20, 38 (1978).

18. R.Ortega-Borges, D.Lincot, *J.Electrochem.Soc.*, 140, 3464 (1993).

19. J.M.Dona, J.Herrero, J.Electrochem.Soc., 144, 4081 (1997).

20. P.K.Nair, P.Parmananda, M.T.S.Nair, *J.Cryst.Growth*, 206, 68 (1999).

21. M.Kostouglou, N.Andritos, A.J.Karabelas, *Ind.Eng.Chem.Res.*, 39, 3272 (2000).

22. C.Voss, Y.-J.Chang, S.Subramanian, S.O.Ryu, T.-J.Lee, C.-H.Chang, *J.Electrochem.Soc.*, 151, 655 (2004).

23. B.E.McCandless, W.N.Shafarman, United States Patent 6,537,845, Mar.25, 2003.

24. D.Lincot, M.Froment, H.Cachet, *Advances in Elcectrochemical Science and Engineering*, Kolb & Alkire (Eds), Wiley.

25. G.Hodes, *Chemical Solution Deposition of Semiconductor Films*, Marcel Dekker, Inc. (Pub) (2003).

26. http://www.rigakumsc.com/xrd/about_tech.html , *XRD theory,* as found on Jan 2nd, 2005.

27. J.P.Sibilia, *Materials Characterization and Chemical Analysis* (1996).

28. http://www.chem.qmw.ac.uk/surfaces/scc/scat5_3.htm, *Photoelectron Spectroscopy,* as found on Dec 16th, 2004.

29. W.J.Danaher, L.E.Lyons, G.C.Morris, *Solar Energy Mater.,* 12, 137 (1985).

30. A.Kylner, M.Wirde, *Jpn.J.Appl.Phys.Part 1,* 36, 2167 (1997).

31. A.Kylner,J.Lindgren, L.Stolt, *J.Electrochem.Soc.,* 143, 2662 (1996).

32. M.Stoev, A.Katerski, *J.Mater.Chem., 6,* 377 (1996).

33. R.D.Seals, R.Alexander, L.T.Taylor, J.G.Dillard, *Inorg.Chem.*, 12, 2486 (1973).

34. http://monet.physik.unibas.ch/famars/afm_prin.htm, *Prniciple of AFM,* as found on Jan 12th, 2005.

35. J.B.Wachtman, *Characterization of Materials* (1993).

36. Institut für Mikrotechnik Mainz, Germany, *Operating manual for SSIMM* (2004).

37. J.Liebig, *Ann.Pharmaz,* 14, 134 (1835).

38. C.Puscher, *Dingl.J.*, 190, 421 (1869).

39. G.Rosenheim,W.Stadler,VJ Mayer,*Z.Anorg.Chem.*, 49, 1 (1906).

40. G.Rosenheim,W.Stadler,VJ Mayer,*Z.Anorg.Chem.*, 49, 13 (1906).

41. S.G.Mokrushin,Y.V.Tkachev,*Kolloidn Zh.*, 23, 438 (1961).

42. H.Uda,H.Taniguchi,M.Yoshida,T.Yamashita, *Jpn.J.Appl.Phys.*, 17, 585 (1978).

43. P.K.Nair, M.T.S.Nair, J.Campos, L.E.Sansores, *Solar cells*, 22, 211 (1987).

44. P.K.Nair, M.T.S.Nair, *Solar Energy Mater.*, 15, 431 (1987).

45. R.C.Bharadwaj, C.M.Jadhav, M.M.Taqui Khan, *Solar Cells*, 12, 371 (1984).

46. S.N.Sahu, S.Chandra, *Solar Cells*, 22, 163 (1987)

47. B.B.Bargale, A.G.Shikalgar, S.H.Pawar, *Thin Solid Films*, 62, 215 (1979).

48. N.R.Pavaskar, C.A.Menzes, A.P.B.Sinha, *J.Electrochem.Soc.*, 124, 743 (1977).

49. A.U.Warad, M.D.Uplane, S.H.Pawar, *Mater.Chem.Phys.*, 13, 91 (1985).

50. C.D.Lokhande, *Mater.Chem.Phys.*, 26, 405 (1990).

51. D.S.Boyle, P.O'Brien, D.J.Otway, O.Robbe, *J.Mater.Chem.*, 9, 725 (1999).

APPENDICES

APPENDIX A

References for Chemical Deposition of Chalcogenides

CdS

a1. C.D.Lockande, *Mater.Chem.Phys.* 28, 145 (1991).

a2. W.J.Danaber, L.E.Lyons, G.C.Morris, *Solar Energy Mater.Solar Cells* 12, 137 (1985).

a3. M.T.S.Nair, P.K.Nair, J.Campos, *Thin Solid Films* 161, 21 (1988).

a4. H.Uda, S.Ikegami, H.Sonomura, *Japanese J.Appl.Phys.*29, 30 (1990).

a5. V.N.Semenov, *J.Appl.Chem.*64, 159 (1991).

a6. T.L.Chu, S.S.Chu, N.Schultz, C.Wang, C.Q.Wu, *J.Electrochem.Soc.* 139, 2443 (1992).

a7. B.R.Lanning, J.H.Armstrong, *Int.J.Solar Energy* 12, 247 (1992).

a8. K.Ito, K.Shiraishi, *Solar Energy Mater.Solar Cells* 35, 179 (1994).

a9. T.Nakanishi, K.Ito, *Solar Energy Mater.Solar Cells* 35, 171 (1994).

a10. L.Hernandez, O.de Melo, O.Zelaya-Angel, R.Lozada-Morales, *J.Electrochem.Soc.* 141, 3238 (1994).

a11. K.Ito. T.Tamaru, *J.Mat.Sci.Lett.* 13, 893 (1994).

a12. N.Andriskos, A.J.Karabelas, *J.Colloid.Interface Sci.* 165, 301 (1994).

a13. S.Gorer, G.Hodes, *J.Phys.Chem.* 98, 5338 (1994).

a14. P.O'Brien, T.Saeed, *J.Crystal Growth* 158, 497 (1996).

a15. I.O.Oladeji, L.Chow, *J.Elcetrochem.Soc.* 144, 2342 (1997).

a16. M.Froment, D.Lincot, *Electrochim.Acta* 40, 1293 (1995).

a17. A.Mondal, T.K.Chaudhuri, P.Pramanik, *Solar Energy Mater.Solar Cells* 7, 431 (1983).

Ag_2S

a18. S.S.Dhumure, C.D.Lockhande, *Thin Solid Films* 240, 1 (1994).

a19. I.Grozdanov, *Semicond.Sci.Technol.* 9, 1235 (1994).

a20. H.Meherzi-Maghraoui, M.Dachraoui, S.Belgacem, K.Buhre, R.Kunst, P.Cowache, D.Lincot, *Thin Solid Films* 288, 217 (1996).

PbS

a21. J.L.Davis, M.K.Norr, *J.Appl.Phys.*, 37, 1670 (1966)

a22. H.Rahnamai, H.J.Gray, J.N.Zemel, *Thin Solid Films*, 69, 347 (1980).

a23. P.K.Nair, M.T.S.Nair, *Semicond.Sci.Technol.* 4, 807 (1989).

a24. P.K.Nair, M.T.S.Nair, A.Fernandez, M.Ocampo, *J.Phys.D:Appl.Phys.*22, 828 (1989).

a25. M.Isshiki, T.Endo, K.Masumoto, Y.Usui, *J.Electrochem.Soc.*137, 2697 (1990).

a26. L.Huang, P.K.Nair, M.T.S.Nair, R.A.Zingaro, E.A.Meyers, *J.Electrochem.Soc.* 141, 2536 (1994).

ZnS

a27. T.G.Leonova, L.F.Bakhturova, V.I.Belyi, S.V.Larionov, N.P.Sysoeva, *Inor.Mat.* 27, 1745 (1991).

a28. R.Ortega-Borges, D.Lincot, J.Vedel, *11th E.C.Photovoltaics Solar Energy Conf.*, H.Stephens & Associates, Bedford (1992), p.862.

a29. J.M.Dona, J.Herrero, *J.Electrochem.Soc.* 141, 205 (1994).

a30. B.Mokili, M.Froment, D.Lincot, *J.Physique IV*, 5, 26 (1995).

CdSe

a31. G.A.Kitaev, T.S.Terekhova, *Russian J.Inorg.Chem.*15, 25 (1970).

a32. R.C.Kainthla, D.K.Pandya, K.L.Chopra, *J.Electrochem.Soc.*127, 277 (1980).

a33. R.A.Boudreau, R.D.Rauh, *J.Electrochem.Soc.* 130, 513 (1983).

a34. G.Hodes, A.Albu-Yaron, F.Decker, P.Motisuke, *Phys.Rev.* B36, 4212 (1987).

a35. A.H.Eid, S.Mahmoud, *J.Mat.Sci.Lett.*11, 937 (1992).

a36. O.Savadogo, K.C.Mandal, *Mater.Chem.Phys.*31, 301 (1992).

a37. J.M.Gracia-Jimenez, G.Martinez-Montes, R.Silva-Gonzalez, *J.Electrochem.Soc.*139, 2048 (1992).

a38. H.Cachet, H.Essaaidi, M.Froment, G.Maurin, *J.Electroanal.Chem.*396, 75 (1995).

APPENDIX B

AFM images of CdS films deposited by batch and CFM

(a)

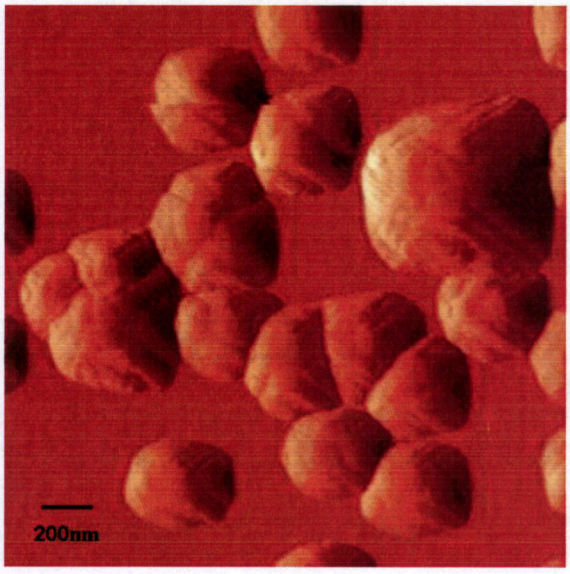

(b)

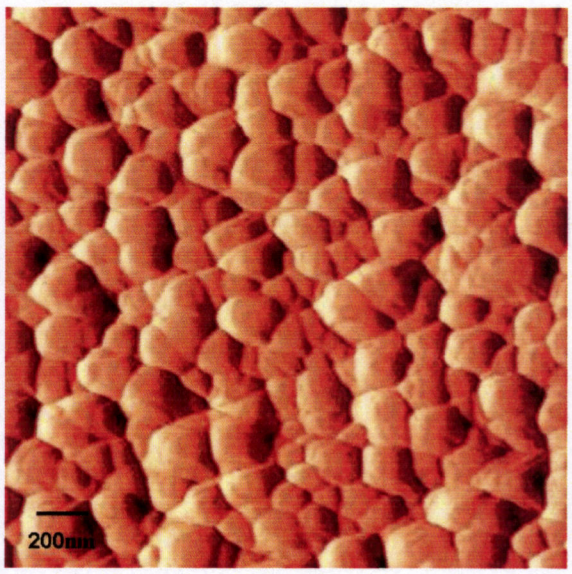

Figure B.1 1 μ m x 1 μ m scan of (a) batch and (b) CFM deposited CdS films

(c)

(d)

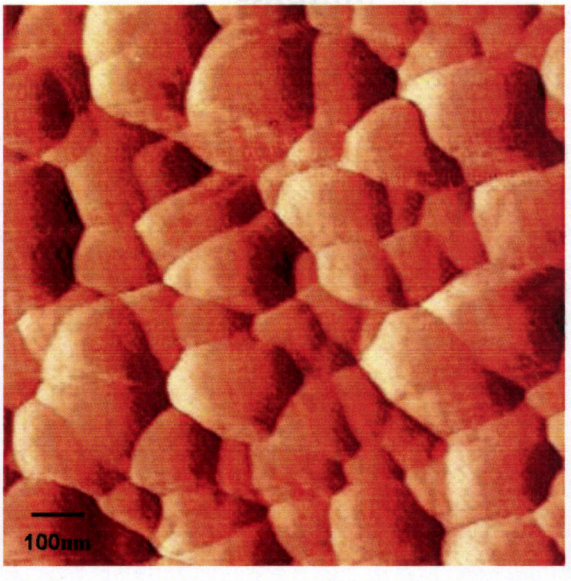

Figure B.2 500 nm x 500 nm scan of (c) batch and (d) CFM deposited CdS films